UM-HSRI-78-53

AN EMPIRICAL MODEL FOR THE PREDICTION OF THE TORQUE OUTPUT OF COMMERCIAL VEHICLE AIR BRAKES

MVMA Project #1.36

L.K. Johnson
P.S. Fancher
T.D. Gillespie

Final Technical Report

December 1978

Highway Safety Research Institute
The University of Michigan
Ann Arbor, Michigan 48109

Technical Report Documentation Page

1. Report No.	2. Government Accession No.	3. Recipient's Catalog No.
UM-HSRI-78-53		

4. Title and Subtitle
AN EMPIRICAL MODEL FOR THE PREDICTION OF THE TORQUE OUTPUT OF COMMERCIAL VEHICLE AIR BRAKES

5. Report Date
December 1978

6. Performing Organization Code

7. Author(s)
L. Johnson, P. Fancher,, T. Gillespie

8. Performing Organization Report No.
UM-HSRI-78-53

9. Performing Organization Name and Address
Highway Safety Research Institute
The University of Michigan
Huron Parkway & Baxter Road
Ann Arbor, Michigan 48109

10. Work Unit No.
361506

11. Contract or Grant No.
MVMA Proj. 1.36

12. Sponsoring Agency Name and Address
Motor Vehicle Manufacturers Association
300 New Center Building
Detroit, Michigan 48202

13. Type of Report and Period Covered
Final
7/1/77-10/15/78

14. Sponsoring Agency Code

15. Supplementary Notes

16. Abstract

An empirical model for representing the torque capability of commercial vehicle brakes is described including discussions of the form of the model, the required test data, and the regression method used to fit the data. Inertial dynamometer data for six pneumatically-actuated brakes are employed in analyses illustrating the application of this modeling technique to brakes of both wedge and S-cam design. The results presented show (1) brake torque divided by actuation effort as a function of sliding speed, interface temperature, actuation force, and work history and (2) the goodness of fit between the empirical model and the original test data. Application of the brake model in a detailed vehicle simulation is discussed. The report concludes with remarks summarizing the properties of the empirical model and recommending research on the influence of work history.

17. Key Words	18. Distribution Statement
brakes, air brakes, interface temperature, work history, brake modeling, processing brake data	UNLIMITED

19. Security Classif. (of this report)	20. Security Classif. (of this page)	21. No. of Pages	22. Price
NONE	NONE	83	

TABLE OF CONTENTS

ACKNOWLEDGEMENTS

The help and support of the following organizations and people are gratefully acknowledged:

The Motor Vehicle Manufacturers Association for project support.

Greening Testing Laboratories and Mr. Robert Hannon for dynamometer tests.

Dave Velliky and Sandy Milazzo for digitizing oscillograph records.

The mechanical technicians at the Highway Safety Research Institute for installing thermocouples.

Jeannette Nafe for typing.

Mr. Percosh Jain of Ford Motor Company and Mr. Thomas Mahaffey of Rockwell International for aid in procurring brake linings.

1.0 INTRODUCTION

Predicting the braking performance of a commercial vehicle in an emergency stop is a very difficult task, requiring detailed information on the vehicle's brakes, antilock system (if it has one), load distribution, suspension characteristics, and tire properties. To aid in predicting and understanding the factors contributing to stopping capability, large-scale, computer-based mathematical models have been developed for simulating emergency braking of commercial vehicles [1]. These large-scale models contain representations of vehicle components (such as the brakes) in separate sections of computer code. The empirical model presented herein is intended to be used as part of a large-scale simulation for studying the influence of measured brake properties on vehicle response during a single stop.

Nonetheless, another important use of an empirical model of brake torque capability is simply to provide a comprehensive summary of the results of numerous dynamometer tests. The form of an example torque versus time curve obtained from a single dynamometer test at a fixed brake line pressure is illustrated in Figure 1.1. In the past, data from a series of tests of the type illustrated in Figure 1.1 have been summarized in graphs of average torque versus initial speed and brake line pressure as shown in Figure 1.2. However, much of the detail of the variation of torque during a stop is lost in working with average torque. In particular, if the conditions for wheel lockup during a stop are to be evaluated, the type of data illustrated in Figure 1.2 is inadequate. Accordingly, values of "peak initial torque," "minimum torque," and "final torque" are sometimes read from curves of the type shown in Figure 1.1. In this regard, the empirical model described here is intended to contain enough information about the brake to essentially reproduce the original torque versus time characteristics.

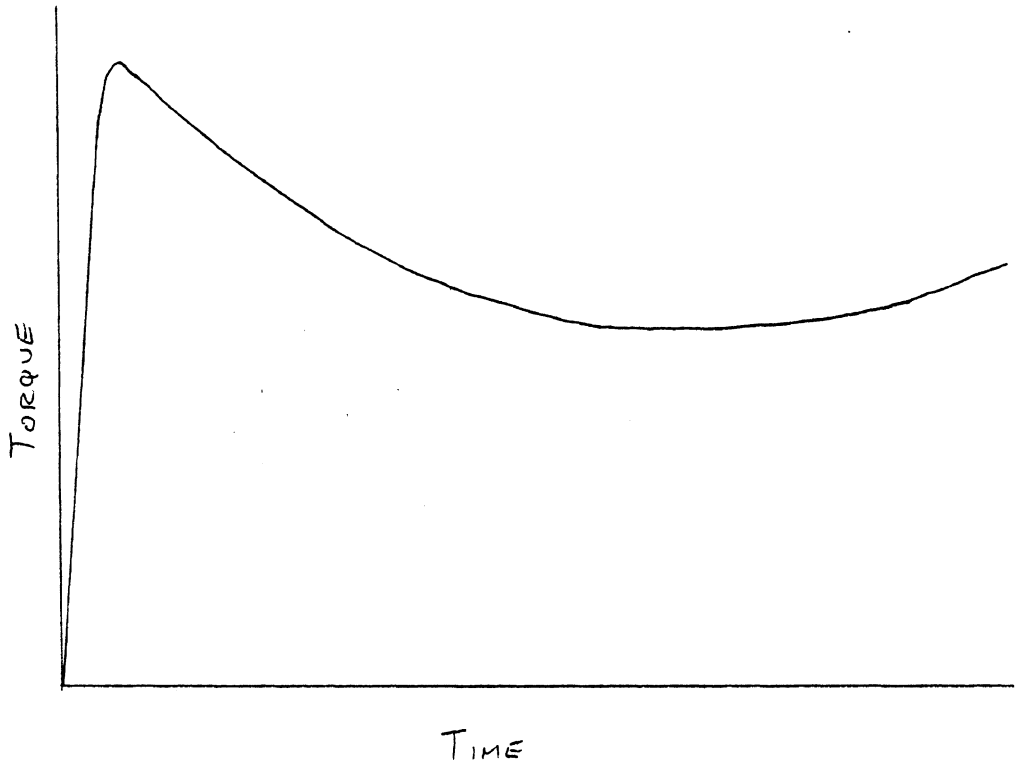

Figure 1.1. Example torque time history from a dynamometer test.

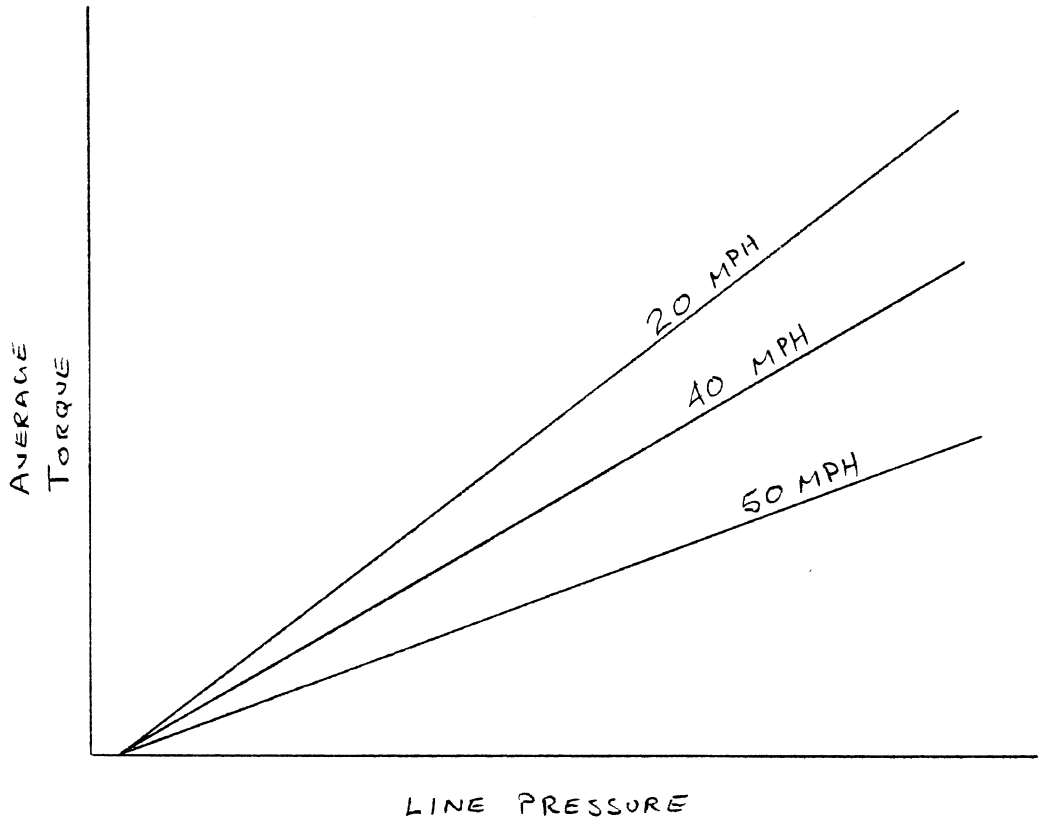

Figure 1.2. Typical summary of average torque versus initial speed and line pressure.

This model was developed following work by H.E. Cook, et al. [2] on passenger car brakes. The independent variables used to predict torque for a brake with a specified prior work history are sliding speed, actuation force (or torque), and interface temperature. The relationship between torque and the independent variables is developed empirically from dynamometer test results.

In addition to predicting stopping distance, other potential applications of the model pertain to predicting (1) brake torque distribution among a vehicle's axles so as to optimize brake system design, (2) wear balance, and (3) mountain descent performance.

This report contains a technical description of the brake model, including discussions of the form of the model, the required test data, and the calculation and regression techniques used to fit the data. Inertial dynamometer data from six pneumatically-actuated brakes are presented and then employed in analyses illustrating the application of this modeling technique to brakes of both wedge and S-cam design with various types of linings. Example results are presented indicating (1) the variation in the "effectiveness function" (i.e., torque output divided by actuation force) as a function of sliding speed, interface temperature, actuation force, and work history and (2) the goodness of fit between the empirical model and the original test data. The body of the report concludes with a brief discussion of the application of this brake model within a large-scale vehicle simulation. Concluding remarks summarizing the properties of this brake model and recommending specific research on the influence of work history appear in a final section.

It is worth noting that the modeling techniques described herein are quite general and they have been employed in another study addressing the torque capability of hydraulically-actuated brakes for heavy trucks [3].

2.0 THE BRAKE MODEL

2.1 The Concept of Brake Effectiveness

It is well known that the frictional characteristics of friction materials are influenced by the temperature, θ, existing at the sliding surface, the sliding speed, V, and the pressure, P, acting between the two elements of the friction pair; i.e., $\mu = \mu(\theta, V, P)$. Thus, it is evident that the torque output of a brake will be dependent on these three factors. However, in the case of a drum brake the dependence will not be linear because of the rather complex geometry relating the coefficient of friction of the lining to the frictional force produced. An example of the sensitivity, s, of brake torque, T, to the coefficient of friction, μ, of the linings for various kinds of drum brakes is shown in Figure 2.1.

$$s = \left(\frac{dT}{d\mu}\right)\left(\frac{\mu}{T}\right)$$

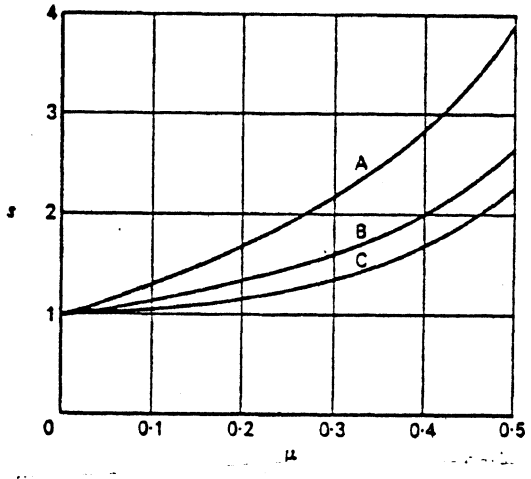

Figure 2.1. Variation of s with μ for different brakes. A: duo-servo; B: two leading shoe (pivoted); C: leading-trailing (pivoted) from Reference [4].

One can create a relationship between the coefficients of friction of the lining and the torque output of the brake per unit force input which is a function of the coefficient of friction and brake geometry. Because μ varies with θ, V, and P, the above relationship will also vary with θ, V, and P. Thus, the torque output of a drum brake can be expressed as follows:

$$T = F\,e \tag{2.1}$$

where T denotes torque output, F denotes the force actuating the shoes, and e denotes torque output per unit force input, which will be called effectiveness for the remainder of this report. Effectiveness, is the parameter which links lining friction to brake torque, and it is a function of θ, V, and P; i.e.,

$$e \equiv e(\theta, V, P) \tag{2.2}$$

However, the pressure acting between the lining and drum is a function of the actuation force, F, so that

$$e \equiv e(\theta, V, F) \tag{2.3}$$

There is one other important factor, ignored up to this point, which affects lining friction, and consequently, effectiveness. That factor is work history, H. Work history is very difficult to quantify, but very easy to observe. An example of the influence of work history is the change in the torque output of a brake after a fade and recovery test compared to the torque output prior to the fade and recovery. Work history, however, can be specified by referring to some portion of a test sequence, e.g., post-burnish effectivenss, first fade, first recovery, final effectiveness, and so on. Therefore, in its final form, effectiveness is defined as

$$e \equiv e(\theta, V, F, H) \tag{2.4}$$

This concept of brake effectiveness, then, treats a brake assembly as a black box with an actuating force being transformed into a torque output. The transfer function, e, is complicated, being a function of interface temperature, sliding speed, actuation force (i.e., pressure between drum and lining), and work history. As a "black box" the brake may be diagrammed as shown in Figure 2.2.

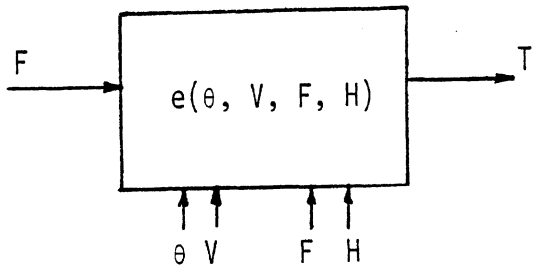

Figure 2.2. A "black box" representation of the mechanical friction brake.

It should be noted that while effectiveness is related to lining friction through the geometry of the brake, there are other factors which play a lesser role. One of these factors is the mechanical efficiency of the actuation mechanism of the brake. Another is compliance of the brake drum and shoes which compliance causes changes in the pressure distribution (across the width of the lining) thus affecting the torque output of the brake. These factors are assumed to be of second-order importance. They are also difficult to quantify, and, therefore, are not explicitly included in the model as variables influencing effectiveness.

2.2 Measuring Effectiveness from Dynamometer Tests

Although the effectiveness function for a particular brake assembly can, in theory, be calculated from known frictional properties of the lining and the geometry of the brake, it is straightforward to measure values of effectiveness from full-scale dynamometer tests. Measuring the performance of a brake as an assembly has the advantage of including effects on the effectiveness function which are inherent in the assembly. Such effects could be systematic or random. For example, the mechanical efficiency of the actuating mechanism would have a systematic effect on the effectiveness function. On the other hand, changes in the pressure distribution across the width of the lining caused by wear, mechanical compliance of the shoe and drum, or thermal distortions of the lining and drum could have both systematic and random effects on the effectiveness function. Thus, it should be expected that measuring

the effectiveness in full-scale tests will yield a more accurate representation of brake performance than can be achieved by calculating effectiveness from frictional properties of linings as measured in tests of lining samples.

Developing the effectiveness function from dynamometer tests requires detailed time histories of the variables involved, because interface temperature and sliding speed are continuously changing throughout a brake application. Additionally, actuation force varies during a constant actuation stop or snub, and brake torque varies during a constant actuation force stop or snub. During a single brake application, effectiveness can be calculated as a function of time with each point in time corresponding to a different temperature, sliding speed, and (possibly) actuation force. Thus, by performing many brake applications over a range of temperatures, sliding speeds, and actuation forces, it becomes possible to map the effectiveness function.

Not only must effectiveness be evaluated at many points during a brake application, but the corresponding values of sliding speed, actuation force, and interface temperature must be known. Whereas sliding speed can easily be computed from instantaneous values of the rotational speed of the brake, the remaining two variables require special attention. For example, in the case of the wedge brake, the force applying the shoes can be computed from known output force characteristics of the air chambers and the wedge angle. On the other hand, the force applying the shoes in a cam brake is not easily computed. However, it is not necessary to know that force. Because the effectiveness model treats the brake as a black box, the actuating force for a cam brake can be considered to be the torque actuating the cam. Cam torque can be computed from known air chamber output force characteristics and the length of the slack adjuster. (Note, then, that effectiveness for a cam brake is computed as $e = T/\tau$ where τ denotes cam torque.)

The temperature that exists at the interface between the lining and drum is extremely difficult to measure. HSRI's experience

with measuring temperatures in brake drums also indicates that the temperature can vary greatly from stop to stop even when stops are made from seemingly identical initial conditions. Additionally, temperatures can vary markedly across the width of the lining. For these reasons, a calculated interface temperature is used in the determination of the effectiveness function. Nevertheless, measured temperatures of the drum at the beginning of a brake application are used as a starting point for calculating the interface temperature. Once a brake application has begun, the interface temperature is calculated using measured values of the instantaneous rate of heat generated at the drum/lining interface. The rate at which heat is generated is merely equal to the product of brake torque and rotational speed. Also, as a simplification, the calculated temperature is the average across the entire width of the lining.

A flow diagram of the procedure used to calculate instantaneous values of effectiveness during a brake application is shown in Figure 2.3.

2.3 Representing the Effectiveness Function

Two methods are available for representing the effectiveness function once a set of data has been generated from dynamometer tests. The first is tabular representation. This method has the advantage of being easily interpreted if a suitable table can be developed. The bounds on the domain of the function are also easily determined by the endpoints for each line of the table. However, a table takes much room to store and, more importantly in this case, can be difficult to construct. Past experience in trying to construct single-valued tables of effectiveness from results of dynamometer tests has proven to be frustrating. Variability in brake test data, inadequate temperature information, and lack of data repeatability due to work-history effects have confounded the situation to the extent that the construction of meaningful tables is extremely difficult.

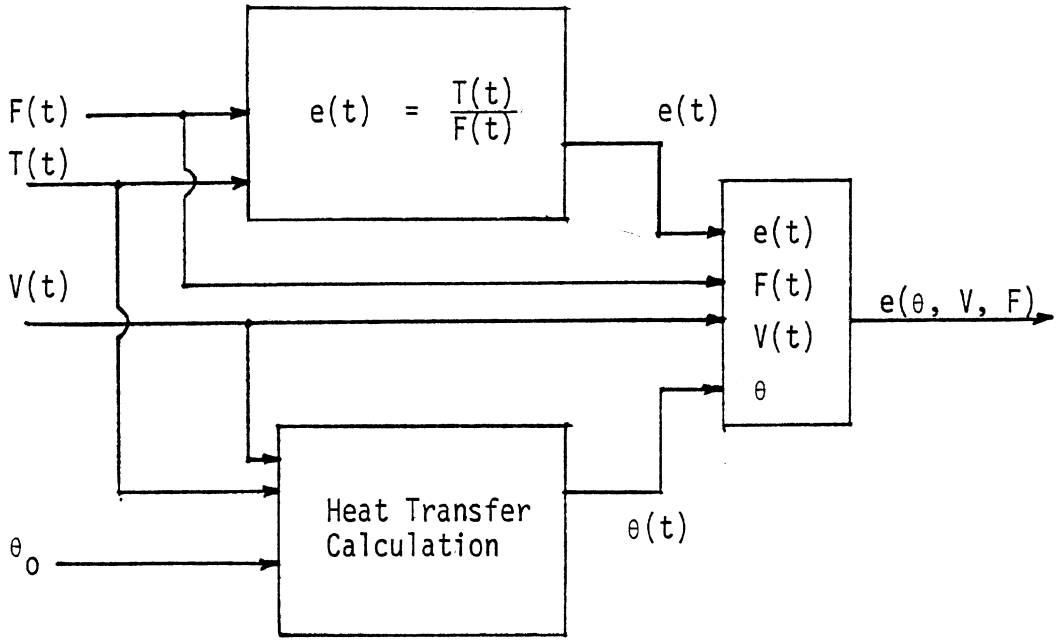

Figure 2.3. Flow diagram for calculating values of effectiveness from dynamometer data (θ_o denotes initial brake temperature).

The second method, and the one chosen for this study, is to employ a curve-fitting process to derive a mathematical equation describing the data.

Since the end use of a brake model is to simulate vehicle braking behavior on a computer, a mathematical description of the effectiveness function is very attractive, because it is better suited for implementation on a computer than a table. Whereas a table requires considerable storage space, an equation only requires storage of some coefficients. The computer can also perform a calculation more quickly than it can a table lookup. Curve fitting the data also smooths the scatter in the data, although sufficient care must be exercised to ensure that the data is not smoothed to the point of eliminating genuine variations.

Curve fitting can also provide two valuable numerics. The first of these is the coefficient of determination, r^2, which represents the fraction of the behavior of the data which the curve fit has described. For example, if a curve-fitting operation produces an r^2 value of 0.9, then the resulting fitted equation explains 90% of the variation of the data. The remaining 10% of unexplained behavior is composed of random errors and errors resulting from systematic trends in the data which the curve fit has ignored.

The second numeric is the standard error. This quantity is a measure of the scatter of the differences between predicted and observed data points. Ideally, it is a measure of experimental error. Thus, the standard error can be used to estimate the range of torques a brake might produce under identical conditions of interface temperature, sliding speed, and actuation force.

A disadvantage of the curve-fitting method is the difficulty of determining the bounds on the domain of the derived effectiveness function. However, this determination can be done, and it is very important to do so as extrapolating a curve-fitted equation can be dangerous indeed.

No attempt is made to represent work history in numerical terms. Rather, for each work history (i.e., post-burnish effectiveness, first fade, etc.) a separate curve-fitting operation is performed. For example, a dynamometer test might consist of several different phases which might be grouped into, say, five work histories. Then, five sets of effectiveness data would be produced and a separate curve-fitting operation performed for each data set. The result would be five curve-fitted equations, each representing the performance of the brake during each of five work histories.

3.0 TEST PROGRAM

3.1 Inertia Dynamometer Tests

Six tests of air-actuated friction brakes were conducted on an inertial dynamometer at Greening Testing Laboratories, Detroit, Michigan. Three tests were conducted on a Rockwell 15 x 6 RDA wedge brake, each test with a different type of lining. The remaining three tests were performed using a Rockwell 16 1/2 x 7 S-cam P brake, also with three different types of lining materials. All of the tests were conducted at a nominal wheel loading of 9000 lbs and a tire radius of 20.2 inches. The inertial load used in these tests was 793 slug-ft^2.

The original-equipment linings used in both the wedge and cam brakes were ABB 693-551D and MM8C5. These lining materials were selected because of their widespread use in FMVSS 121 air brake systems. Other linings tested were the Euclid E84 (in the wedge brake) and Euclid E80 (in the cam brake). These latter linings are aftermarket linings, and although they are slightly different formulations, they are recommended for equivalent applications.

The wedge brake was actuated by two Type 16 air chambers and used a 10° wedge angle. A Type 30 air chamber and a 6-inch slack adjuster length was used on the cam brake.

The brakes and linings tested are summarized in Table 3.1.

All six tests followed the same procedure, which was similar to an FMVSS 121 dynamometer test. The test consisted of three parts: burnish, post-burnish effectiveness, and fade and recovery. Effectiveness data is thus acquired for three work histories: (1) post-burnish effectiveness, (2) fade, and (3) recovery.

The effectiveness test differs somewhat from the 121 procedure in that it is designed to cover a broad range of temperatures and sliding speeds so that a sufficient amount of data could be generated to

Table 3.1. Brakes and Linings Tested.

Brake Assembly	Linings
Rockwell 15 x 6 "RDA" Wedge	ABB 693-551D
Gunite 2046A Drum	MM8C5
Type 16 Air Chambers 10° Wedge Angle	E84
Rockwell 16 1/2 x 7 "P" S-Cam	ABB 693-551D
Gunite 3166 Drum	MM8C5
Type 30 Air Chamber 6" Slack Adjuster	E80
Wheel Load - 9000 lbs	
Tire Radius - 20.2 in	
Inertia - 793 slug-ft^2	

determine an effectiveness function. For this reason, the effectiveness test consisted of five stops made from 30 mph at initial brake temperatures (IBT's) of 150, 200, 250, 300, and 350°F, followed by five stops from 50 mph at the same initial brake temperatures. These stops were run in a constant pressure mode at a pressure which was determined to yield an average deceleration of 12 fpsps for stops from 30 and 50 mph at an initial brake temperature of 150°F. Therefore, data was only generated for two levels of actuation force. Although it would have been desirable to test over several levels of actuation force, insufficient dynamometer time was available for this purpose.

The fade and recovery test, also, differed somewhat from a 121 procedure. Instead of constant deceleration applications as

specified by 121, constant pressure applications were used. Otherwise, the procedure was the same: ten fade snubs starting at 175°F, followed by a hot stop, followed by 20 recovery stops. The details of the test procedure are contained in Appendix A.

The variables recorded during each test were: (1) brake torqure, (2) wheel speed, (3) line pressure, (4) air chamber stroke, and (5) drum temperature at four locations. These variables were recorded on an oscillograph for each brake application.

Three thermocouples were installed in each drum with their measuring junctions positioned approximately 0.040" below the braking surface. One thermocouple was placed in the center of the rubbing path while the other two were placed one inch in from either edge of the lining. These thermocouples were used in an attempt to measure the temperature at the drum/lining interface. It is necessary to place a thermocouple in the drum rather than the lining to meet this objective because approximately 95% of the heat generated during braking flows into the drum with typical organic linings and cast iron drums [4]. The standard SAE lining thermocouple is a poor indicator of interface temperature. Placing three thermocouples across the width of the lining also allowed observations of temperature variations across the lining. The thermocouples worked very well throughout all of the tests.

The construction of these drum thermocouples is shown in Figure 3.1. Originally designed at the University of Illinois for passenger car brake drums [3], they were adapted at HSRI for use in commercial vehicle brake drums. They are of a 1/4" diameter plug-type construction which is pressed into a through-hole drilled in the drum, and afterwards ground flush with the braking surface.

The fourth drum temperature was measured by a thermocouple welded to the periphery of the drum opposite the center of the rubbing surface.

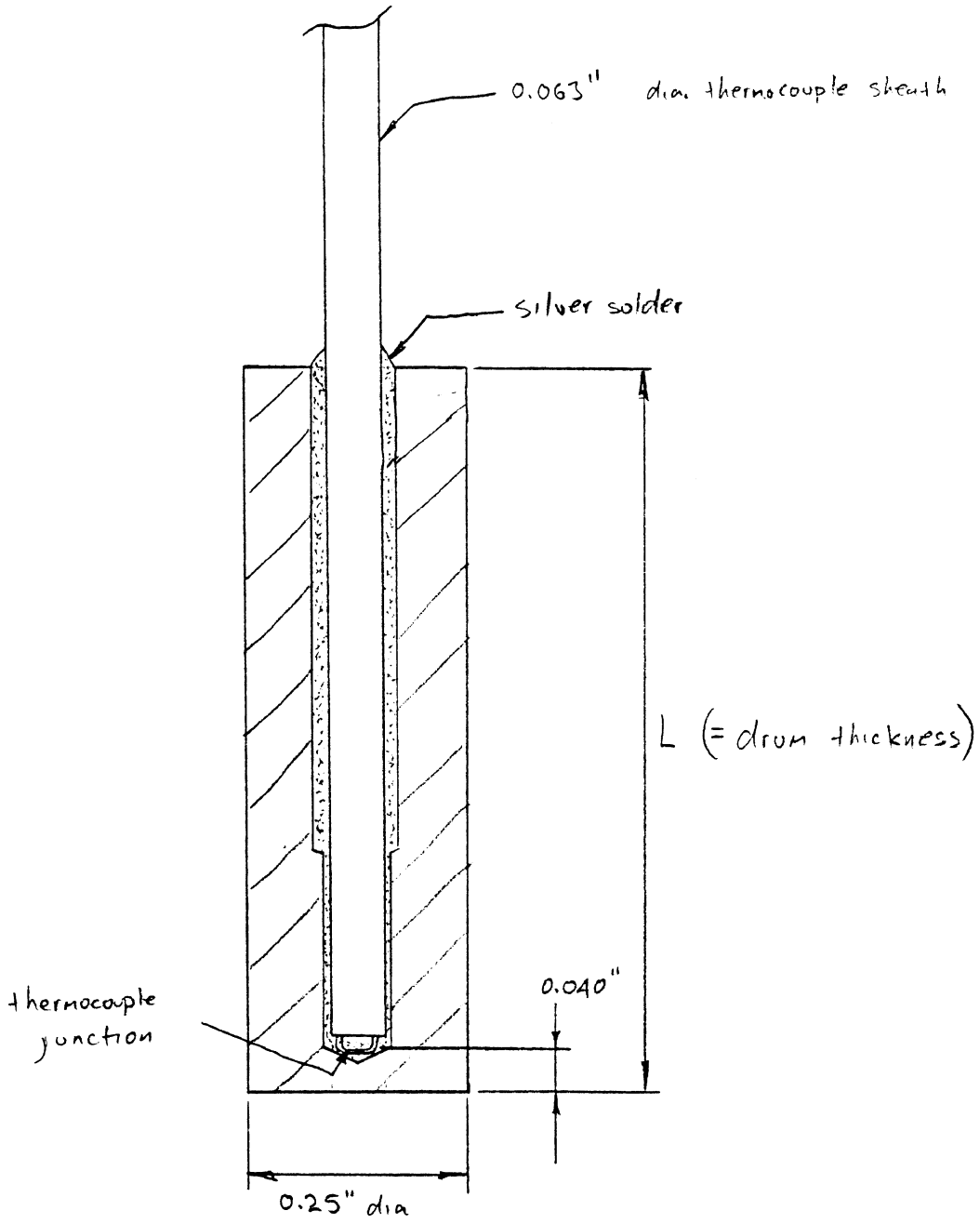

Figure 3.1. Schematic of plug-type thermocouple construction.

3.2 Processing of the Raw Data

To derive the effectiveness function from the time histories recorded during test, the oscillograph recordings obtained during each brake application were semi-automatically digitized on an X-Y table. A cursor on the table is moved by hand over each data trace while points along the trace are sampled and digitized into X-Y coordinates. The digitized points are automatically written into a computer file. For each brake application, the file contains a digitized record of each data trace, along with time scale information, beginning and ending points for the application, and zeros for each trace.

The information in each file is subsequently processed by computer program TRANSLATE. TRANSLATE reads the information stored in a file and translates it into physical units. The program produces two outputs. The first is a printed record for each brake application containing a record of the application at 20 equally spaced points. Also, some summary information is printed such as average torque and pressure, initial and final speeds, etc. A sample page of output is shown in Figure 3.2. The second form of output is a very detailed record of each application which is written on magnetic tape. This tape is later analyzed by program DYNA-DRUM III which calculates the values of effectiveness at a series of points during each application.

3.3 Torques Achieved During Each Test

The minimum and maximum values of torque achieved during the effectiveness portions for each test are shown in Figures 3.3a-c and 3.4a-c for each brake and lining combination tested. The range of torques experienced during the fade and recovery cycle is shown in Figures 3.5a-c and 3.6a-c, again for each brake and lining combination.

The figures show that the variation of torque within a stop is much greater for the wedge brake than it is for the cam brake. This

ROCKWELL 16-1/2 X 7 S-CAM BRAKE ABB 693-551D LINING
MVMA PROJECT #1.36 GREENING TESTING LABS TEST M2-13-15 13 JULY,1978
POST-BURNISH EFFECTIVENESS

STOP 8 50 MPH 250 DEG F

	TIME (SEC)	PRESSURE (PSI)	STROKE (IN)	SPEED (MPH)	TORQUE (K IN-LBS)	TEMPERATURES (DEG F) SURFACE 1	SURFACE 2	SURFACE 3	PERIPHERY
1	0.0	3.8	0.54	51.2	2.7	224	250	224	242
2	0.29	34.3	1.28	48.8	77.4	242	252	232	242
3	0.58	34.0	1.29	46.4	75.9	256	260	250	240
4	0.88	34.3	1.28	43.8	73.5	264	274	268	240
5	1.17	34.0	1.29	41.2	71.4	268	290	286	240
6	1.46	34.3	1.30	38.6	70.2	274	308	300	242
7	1.75	34.0	1.30	36.0	69.3	276	324	310	242
8	2.04	34.0	1.32	33.6	68.7	274	336	318	242
9	2.34	34.0	1.31	31.0	68.7	274	348	328	244
10	2.63	34.3	1.33	28.6	68.4	276	360	338	248
11	2.92	34.0	1.34	25.8	67.8	280	370	342	252
12	3.21	34.0	1.36	23.4	68.1	282	376	346	260
13	3.51	34.0	1.36	21.2	68.7	286	378	350	264
14	3.80	34.0	1.36	18.6	69.6	288	386	352	268
15	4.09	34.0	1.36	16.2	70.2	292	392	352	274
16	4.38	34.3	1.37	13.6	71.1	296	396	352	278
17	4.67	34.5	1.37	11.2	71.7	300	398	352	284
18	4.97	34.5	1.37	8.8	72.9	302	400	356	290
19	5.26	34.5	1.37	5.6	73.5	304	400	358	296
20	5.55	34.5	1.38	2.8	73.8	306	402	358	300
21	5.84	34.5	1.39	0.6	76.8	306	402	356	306

STOP TIME: 5.84 SEC

AVG PRESSURE: 33.5 PSI

SPEED
  INITIAL: 51.2 MPH
  FINAL: 0.6 MPH

AVG STROKE: 1.32 IN

TORQUE
  MAX: 78.3 K IN-LBS
  MIN: 68.1 K IN-LBS
  AVG: 69.9 K IN-LBS

TEMPERATURES (DEG F)

	INITIAL	MAX	RISE
SURFACE 1	224	306	82
SURFACE 2	250	402	152
SURFACE 3	224	358	134
PERIPHERY	242	306	64

Figure 3.2. Sample output from program TRANSLATE.

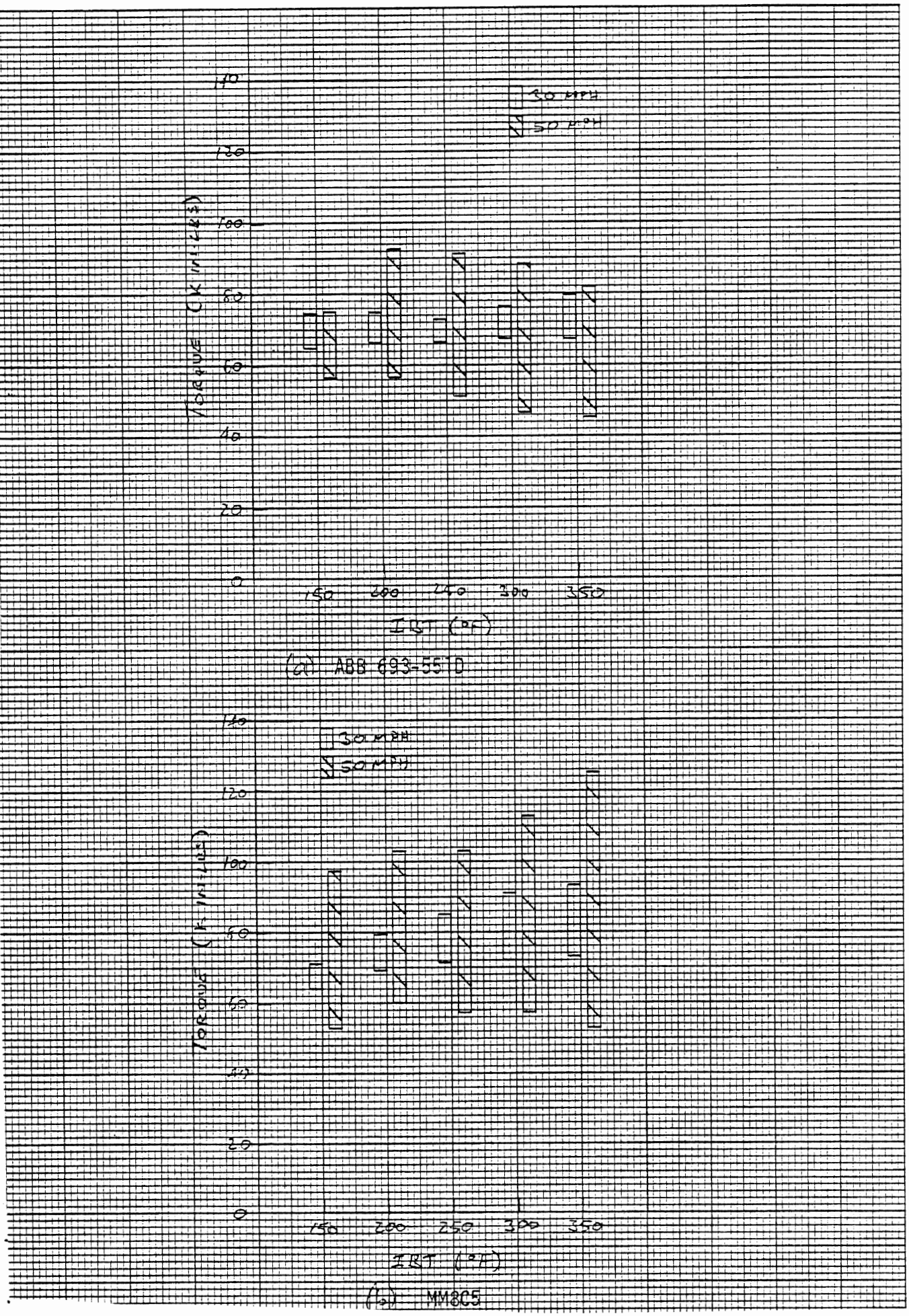

Figure 3.3. Minimum and maximum torques achieved during the post-burnish effectiveness - 15 x 6 wedge.

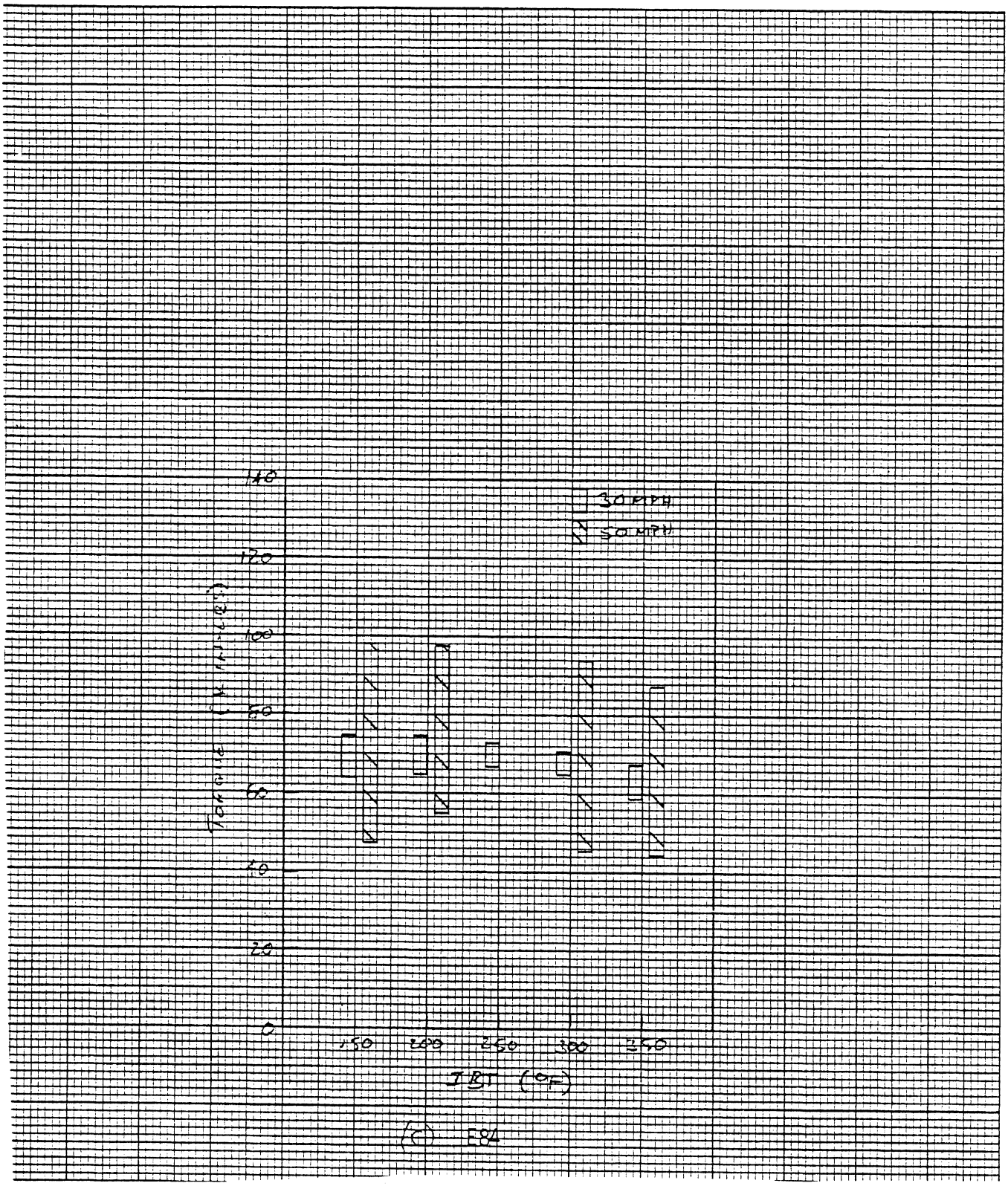

Figure 3.3 (Cont.)

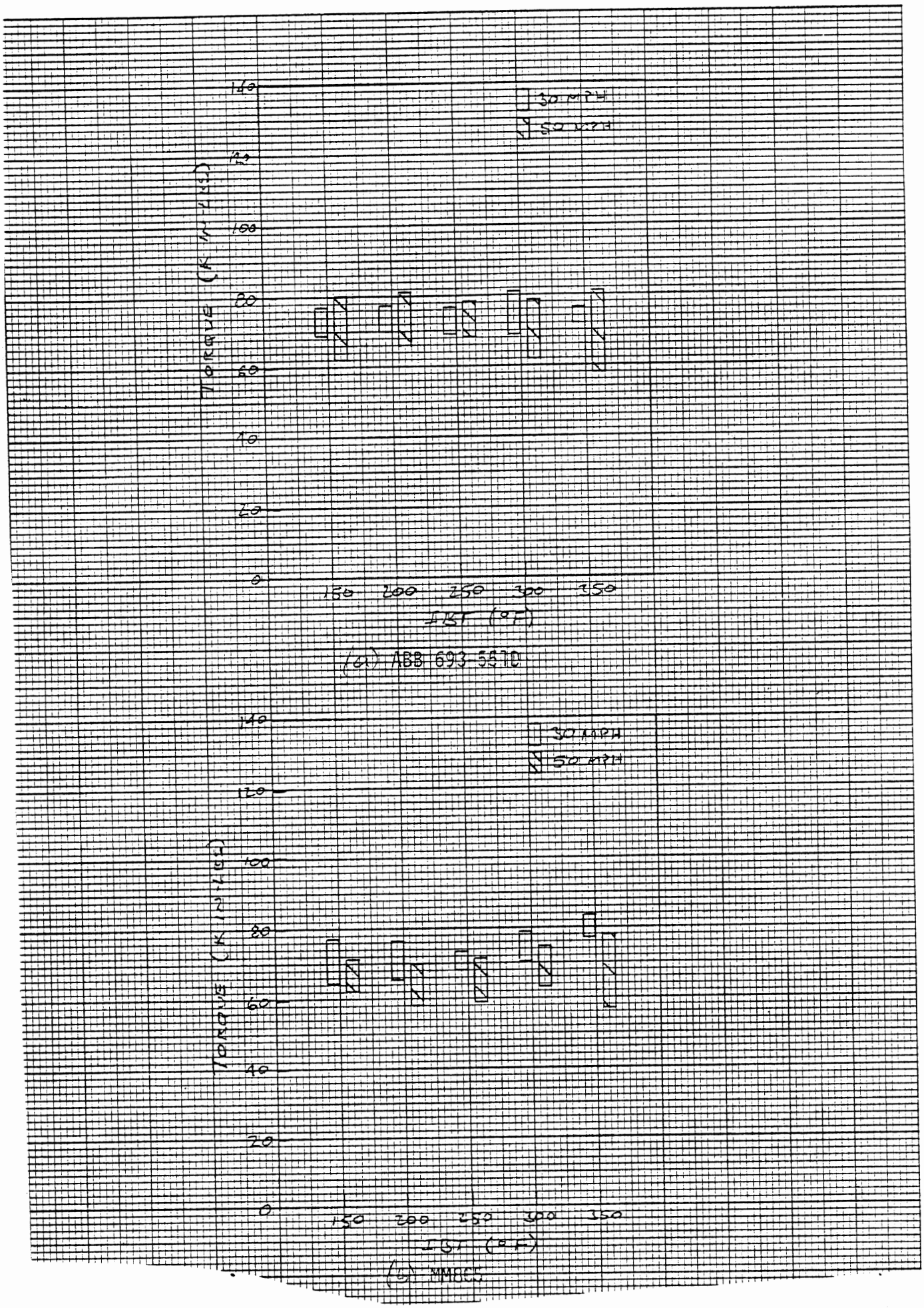

Figure 3.4. Minimum and maximum torques achieved during the post-burnish effectiveness - 16 1/2 x 7 S-cam.

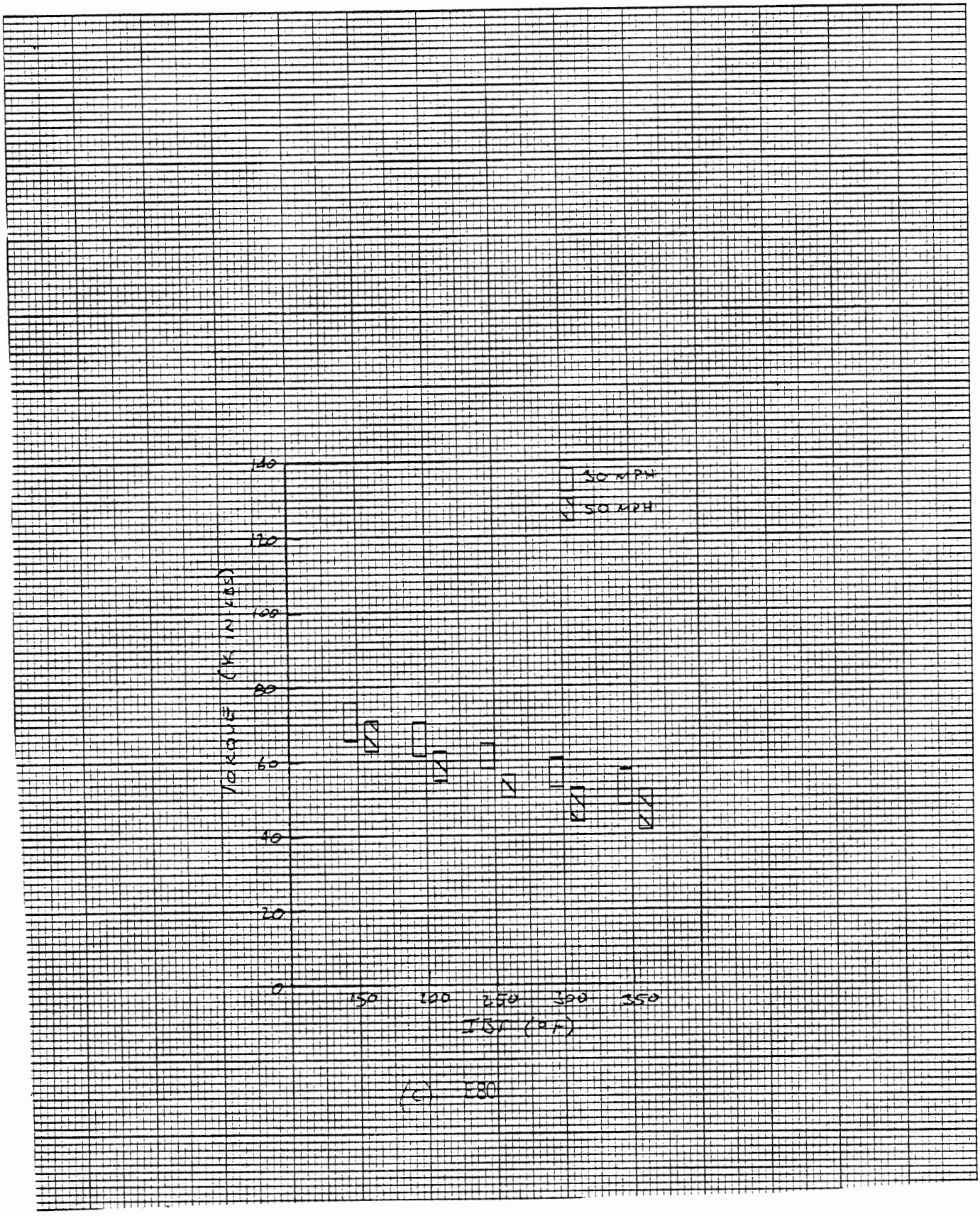

Figure 3.4 (Cont.)

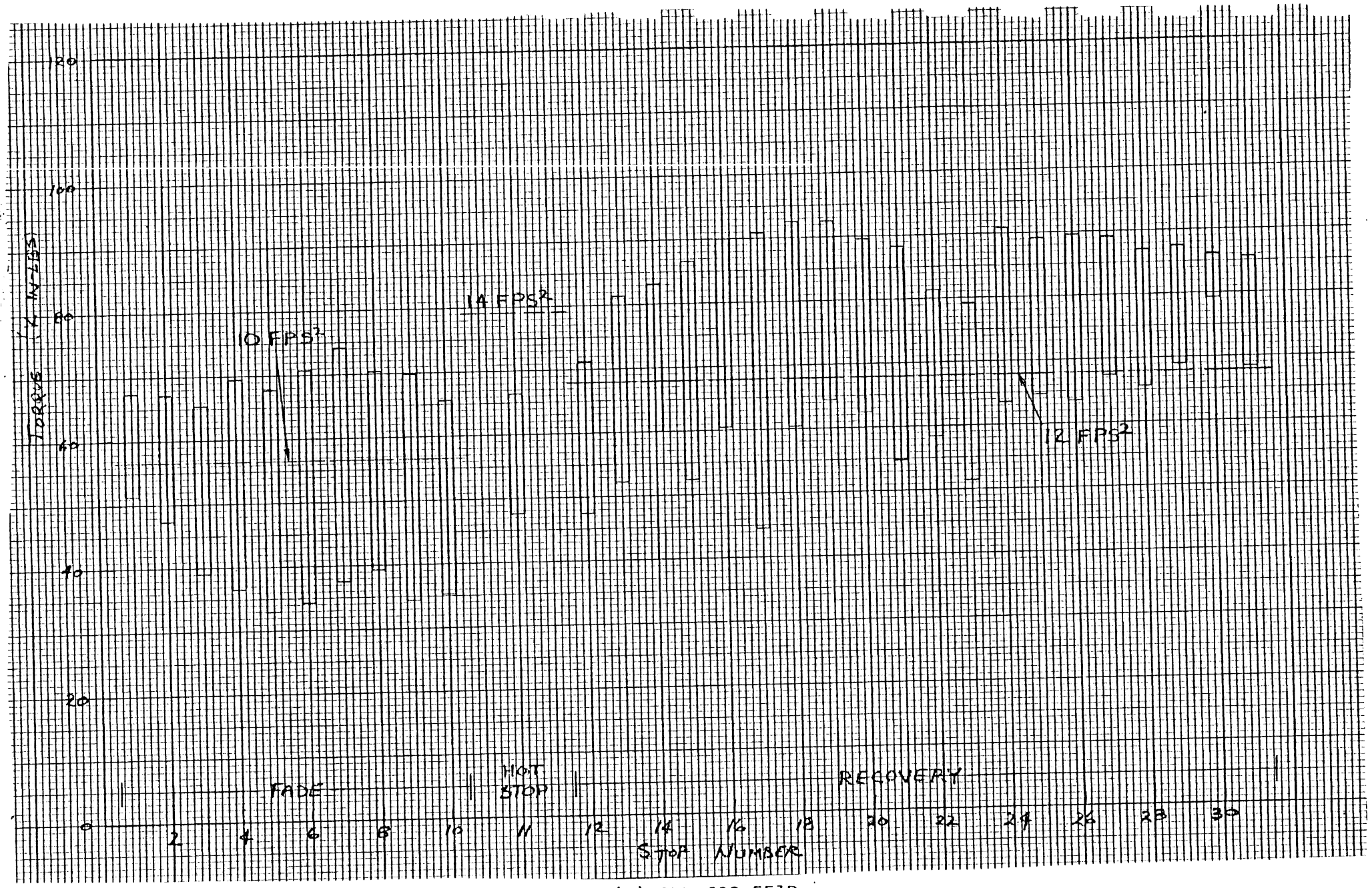

(a) ABB 693-551D

Figure 3.5. Minimum and maximum torques achieved during the fade recovery - 15 x 6 wedge.

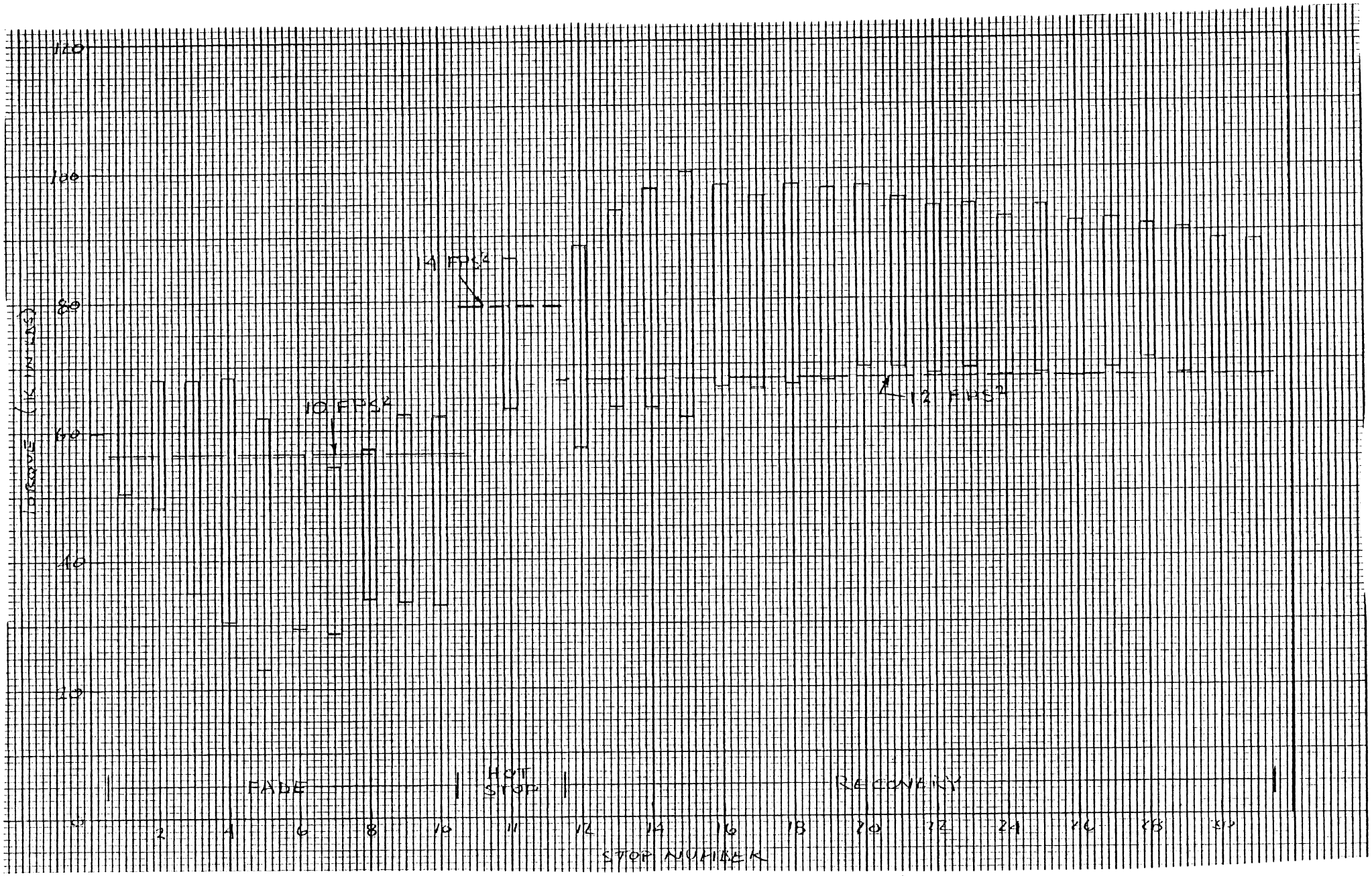

(b) MM8C5

Figure 3.5 (Cont.)

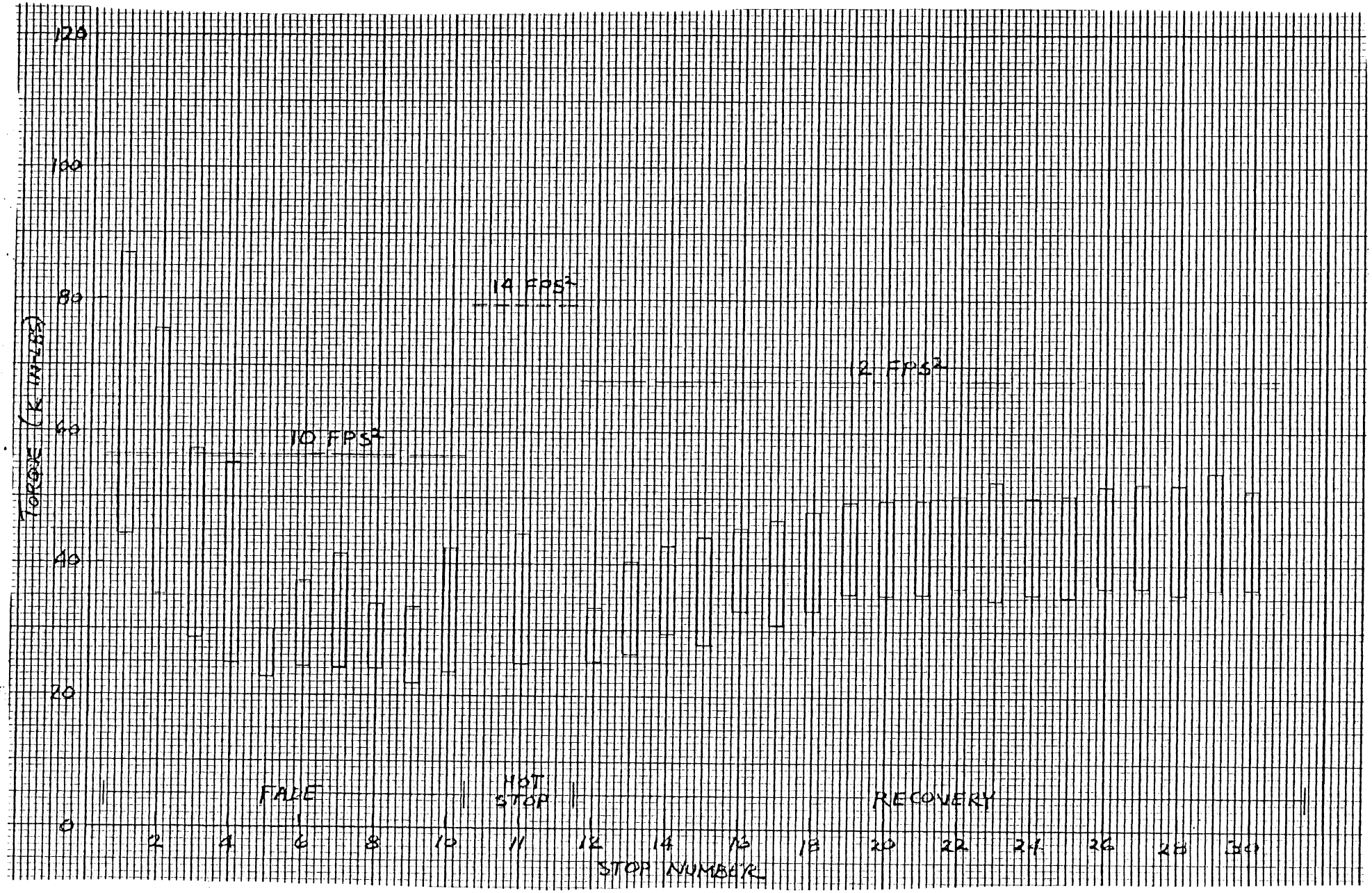

(c) E84

Figure 3.5 (Cont.)

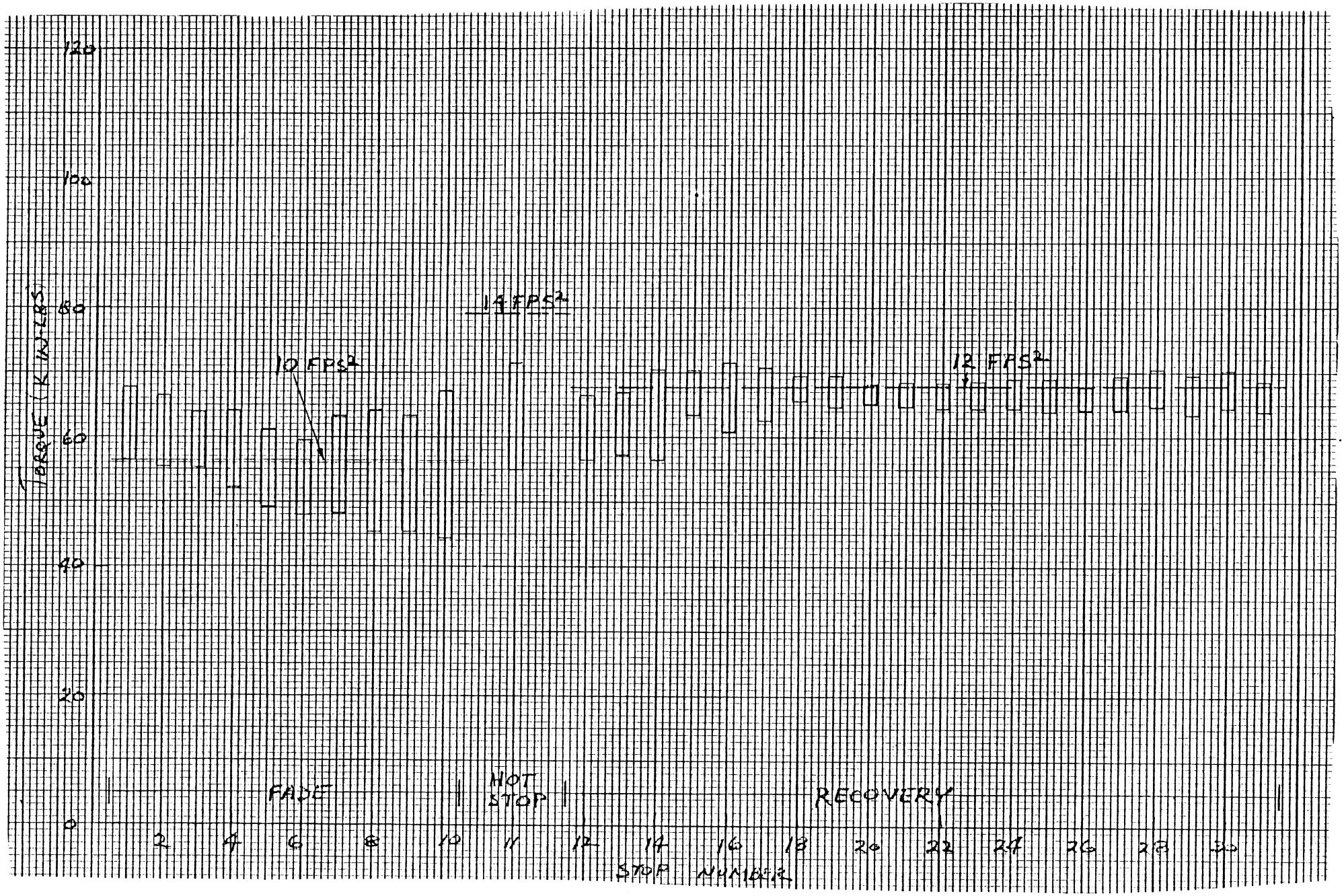

(a) ABB 693-551D

Figure 3.6. Minimum and maximum torques achieved during the fade and recovery - 16 1/2 x 7 S-cam.

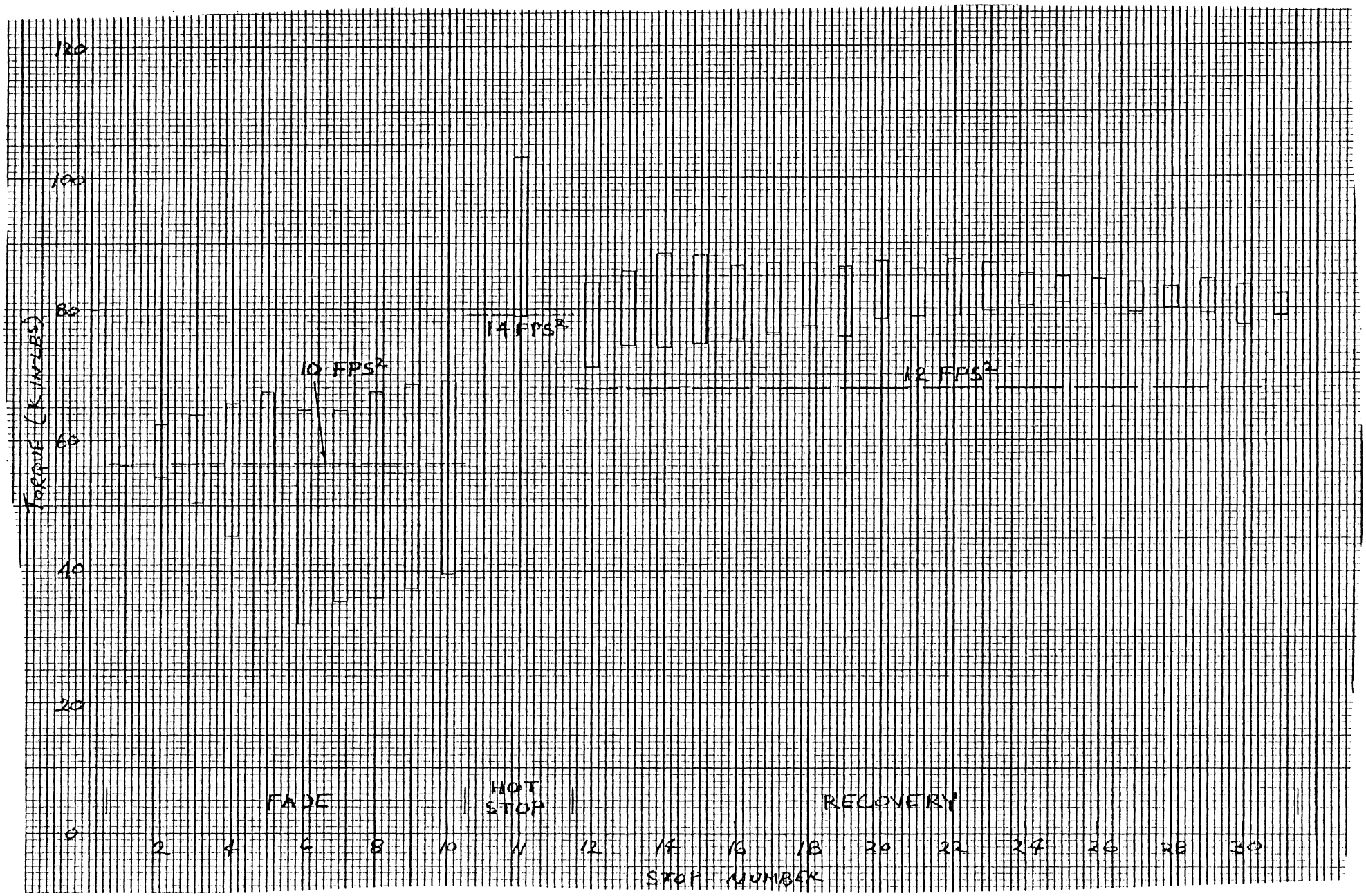

(b) MM8C5

Figure 3.6 (Cont.)

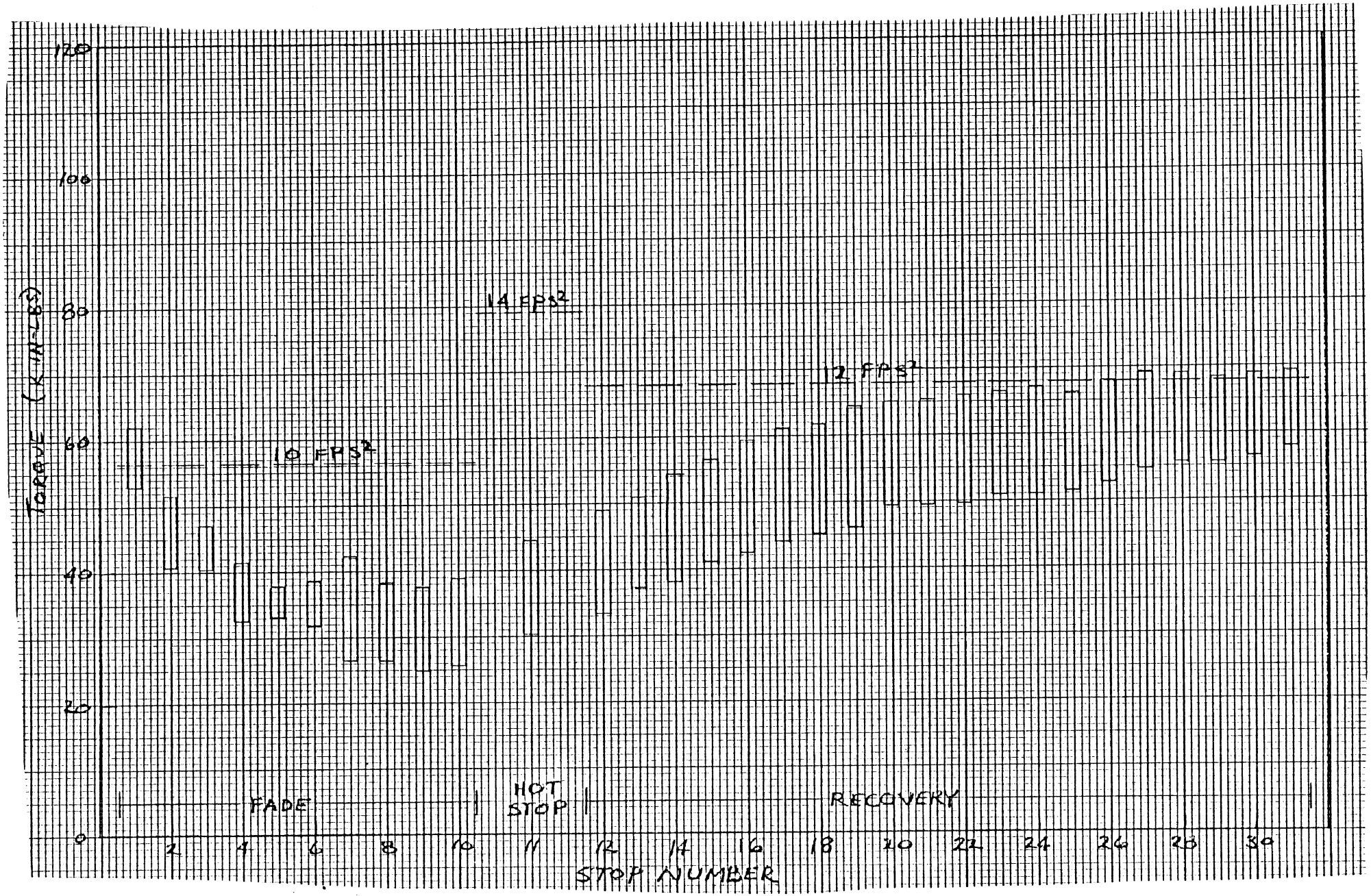

(c) E80

Figure 3.6 (Cont.)

behavior indicates that the wedge brake is more sensitive to changes in the coefficient of friction than is the cam. This behavior is expected because the wedge brake has two leading shoes, which is a configuration more sensitive to changes in μ than the leading-trailing shoe construction of the cam brake.

The effects of temperature on brake torque output are evident, in particular, in the data obtained in the fade and recovery tests (Figures 3.5 and 3.6). As temperature rises, with each successive fade snub, torque falls. The E80 and E84 linings are especially graphic in this regard. And as the brakes cool during the recovery, torque begins to rise again. In fact, the brake may actually become more effective toward the end of the recovery than it was prior to the start of the fade. This behavior is demonstrated by the MM8C5 lining in both brakes. The effect of work history is illustrated by this phenomenon—namely, the brake has changed between the start of the fade cycle and the end of the recovery cycle.

4.0 DATA ANALYSIS - DERIVING THE EFFECTIVENESS FUNCTION

4.1 Calculating Effectiveness for Wedge and Cam Brakes

At each instant during a brake application a value of effectiveness may be calculated corresponding to the instantaneous values of interface temperature, sliding speed, and actuation force occurring at that time. Recalling that effectiveness is defined as torque output divided by actuation force, effectiveness for a wedge brake can be calculated from Equation (4.1):

$$e = \frac{T}{\left(\frac{F_{AC_1} + F_{AC_2}}{2} - S_w\right)\frac{1}{2}\cot\frac{\alpha}{2}} \tag{4.1}$$

where $F_{AC_{1,2}}$ denotes the force produced by the two air chambers, S_w denotes the force required to overcome the return springs, and α denotes the included angle of the wedge.

For a cam brake, the force applying the shoes is replaced by the torque actuating the cam. Therefore, effectiveness is calculated as

$$e = \frac{T}{F_{AC}\ell - S_c} \tag{4.2}$$

where F_{AC} denotes the force produced by the air chamber, ℓ denotes the length of the slack adjuster, and S_c denotes the torque required to overcome the return springs.

4.2 Determining the Force Produced by the Air Chambers

Although the force produced by an air chamber is highly linear with pressure, it is decidedly nonlinear with stroke. Graphs of the behavior of the output force for a typical air chamber are shown in Figures 4.1a and b. Because it is necessary to know the force

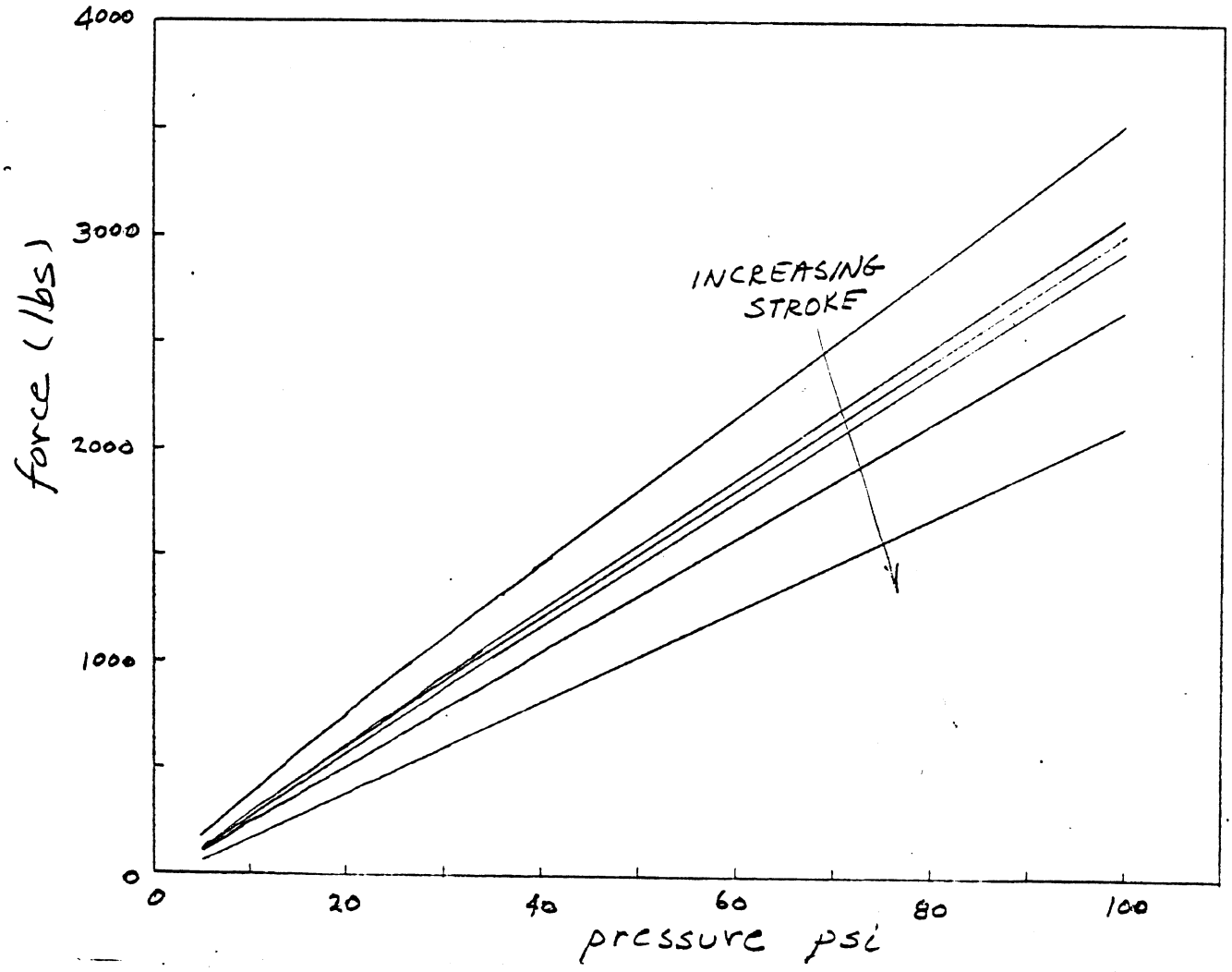
4000
3000
2000
1000
0
force (lbs)
INCREASING
STROKE
0
20
40
60
80
100
pressure psi

(a)

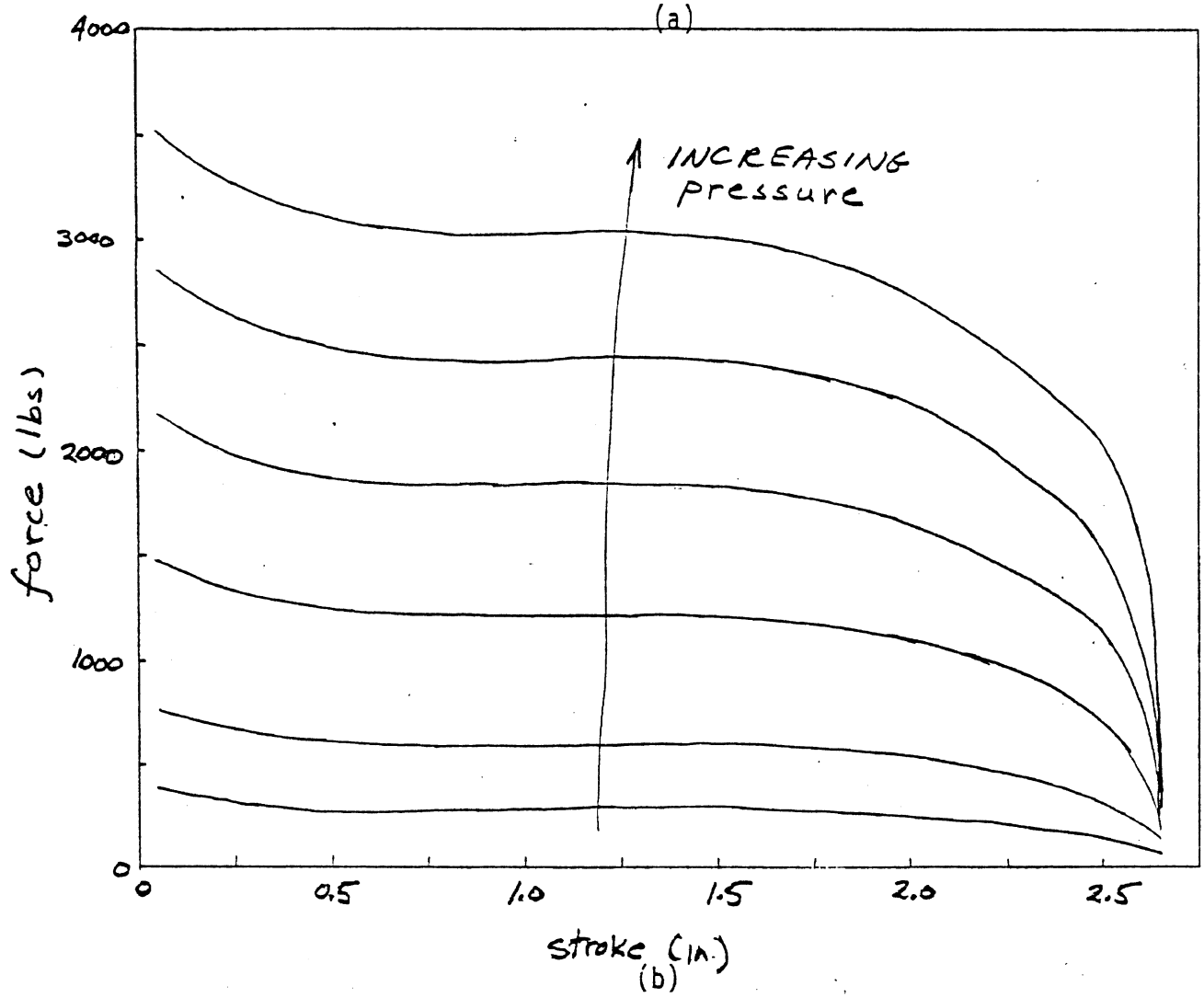
4000
3000
2000
1000
0
force (lbs)
INCREASING
pressure
0
0.5
1.0
1.5
2.0
2.5
stroke (in.)

(b)

Figure 4.1

produced by the air chambers for calculating effectiveness, the output force characteristics of the air chambers used in the dynamometer tests were evaluated with the aid of a test fixture previously constructed at HSRI. This fixture uses a load cell to measure the output force of the air chamber while the line pressure and stroke are varied over the operating range of the air chamber.

Although the performance of the air chambers tested was virtually independent of stroke in the vicinity of the mid-range of stroke, one cannot guarantee that an air chamber will always operate in this range. In fact, the air chambers were not always operating in this range during the dynamometer tests. Therefore, for purposes of calculating the output force for the effectiveness calculations, the air chambers were characterized over their entire operating range. It was found that the output force could be represented as varying in a linear manner with pressure and in a cubic manner with stroke. Thus, equations of the form

$$F = \sum_{i=1}^{2} \sum_{j=1}^{3} a_{ij} p^{i-1} x^{j-1} \qquad (4.3)$$

(where p denotes pressure and x denotes stroke) were determined for each air chamber by a least-squares regression. For the Type 16 chamber, a least-squares regression yielded the following equation:

$$\begin{aligned} F = {} & 57.290 + 20.329p - 380.28x - 10.974px \\ & + 505.87x^2 + 11.135px^2 - 184.15x^3 \\ & - 3.9664px^3 \end{aligned} \qquad (4.4a)$$

and for the Type 30 air chamber:

$$F = 53.686 + 35.631p - 200.53x - 13.973px + 172.19x^2 + 12.476px^2 - 45.095x^3 - 3.7117px^3 \quad (4.4b)$$

These equations describe the measured behavior of each air chamber extremely well.

4.3 Return Spring Efforts

The force or torque which must be exerted to overcome the return springs is a factor which is difficult to estimate accurately because of the difficulty of determining just when the linings are brought into contact with the drum. Furthermore, it is a factor which can vary somewhat because of (1) changes in thickness of linings and (2) brake adjustment. However, it is not necessary to know this quantity with great precision because it is not a large factor in the net actuation force or torque.

Return spring efforts were estimated from the oscillograph charts by observing the line pressure and stroke at the instant the brake torque began to rise. Then the return spring force or torque could be calculated with the aid of Equations (4.1) or (4.2). A slight step in the pressure trace occurs at the time the brake torque begins to rise, and, typically, about 5 psi were required to overcome the return springs. Table 4.1 lists the return spring efforts which were estimated for each of the tests.

Table 4.1. Values of Return Spring Forces and Torques.

Brake	Lining	Return Spring Force or Torque
15 x 6 wedge	ABB 693-551D	90 lbs[1] 80 lbs[2]
	MM8C5	80 lbs
	E84	60 lbs
16 1/2 x 7 S-cam	ABB 693-551D	900 in-lbs
	MM8C5	750 in-lbs
	E80	500 in-lbs

[1] post-burnish effectiveness

[2] fade and recovery

4.4 Calculating Sliding Speed

Sliding speed can easily be calculated at any instant during a brake application from the wheel rotational speed and the radius of the drum, i.e., $v = \omega r$. In these tests, the rotational speed of the drum was not recorded, per se, but the equivalent road speed of the wheel was. Therefore, sliding speed, v, can be calculated as

$$v = V\left(\frac{88}{60}\right)\frac{r}{R}\ , \text{fps} \qquad (4.5$$

where V denotes road speed in mph, r denotes drum radius, and R denotes tire radius.

4.5 Calculating Interface Temperature

A finite-element heat-transfer model of the brake drum is used to calculate the temperature at the interface between the drum and lining. The model assumes heat flow in radial and axial directions, but none in a circumferential direction. Also, a constant heat flux input across the width of the braking surface is assumed. The heat transfer model adopted to represent the 16 1/2 x 7 drum is illustrated in Figure 4.2. (The model adopted to represent the 15 x 6 drum is essentially identical, except for different dimensions.) The mounting flange of the drums, which would extend downward to the left in the figure, has been ignored. Calculations showed that very little heat actually flows into the mounting flange during a single snub or stop. Ignoring the mounting flange has a miniscule effect on the temperature calculated at the braking surface.

The temperature calculation is exercised by supplying a time history of the rate of heat being input to the drum. Temperature calculations are made at time increments of 0.05 second for the two drum models. The rate of heat input to the drum is defined as:

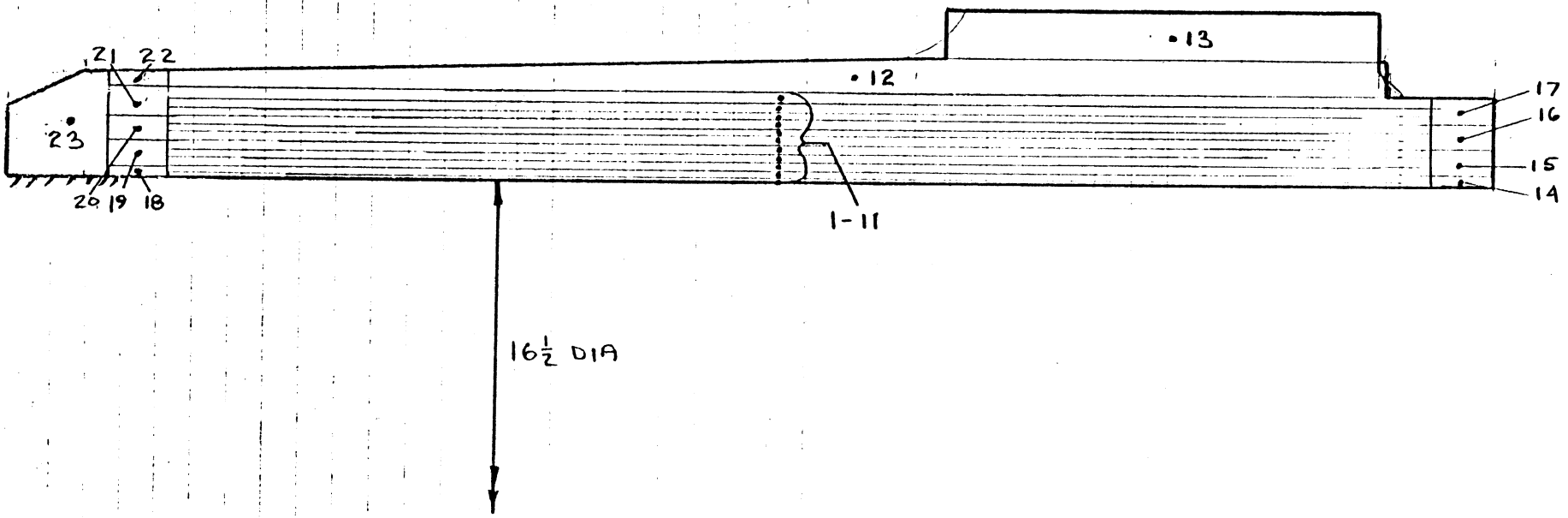

Figure 4.2. Cross-section through 16 1/2 x 7 brake drum showing the finite-element nodes.

$$g = \frac{\sigma T_\omega}{A} \tag{4.6}$$

where σ denotes the fraction of the heat generated which enters the drum, and A denotes swept area. A value of 0.95 was used for σ. This value is quite representative for brakes having organic linings and cast iron drums.

In addition to the rate of heat input, the temperature calculation also requires a starting point—the temperature of the drum at the start of the brake application. The average of the three temperatures indicated by the sub-surface drum thermocouples at the initiation of the brake application is used for this value. By the time the brake has cooled to the point where another application can be made, the temperatures measured by the three thermocouples are approximately the same. For the temperature calculation, all the nodes are initialized to this average temperature.

Values of the thermal conductivity and thermal diffusivity of the drum material are also required by the calculation. The value of thermal conductivity used was 30 BTU/hr-ft/°F, while the value of thermal diffusivity used was 0.43 ft^2/hr. These values are similar to values used by other investigators [4,5,6], and they do provide a reasonable match between calculated and measured temperatures. Very precise knowledge of these parameters is not necessary because the temperature calculation is not highly sensitive to changes in these factors.

The thermal model also allows convective heat transfer to take place at the periphery of the drum. Heat transfer coefficients were therefore estimated from cooling curves from the temperature measured at the drum periphery. For the wedge brake tests, the heat transfer coefficient was estimated to be 17 BTU/hr/ft^2/°F, and for the cam brake tests, 19 BTU/hr/ft^2/°F. The cooling curves were obtained with the brake rotating at 30 mph. Calculations show that very little cooling takes place during a typical brake

application, and so accurate knowledge of the heat transfer coefficient is unnecessary. In fact, while there may be some cooling effect at the periphery of the brake during an application, the temperature at the braking surface is not affected.

4.6 Computer Program DYNA-DRUM III

All of the computational elements discussed in Sections 4.1 through 4.5 are assembled in a computer program called DYNA-DRUM III. The program reads all of the parameters describing the brake, and then performs calculations of drum temperature, sliding speed, actuation force/torque, and effectiveness for a set of brake applications. The digitized time histories produced by program TRANSLATE are used as input.

The output exists in two forms. One is a printed record of each brake application for 22 points in time during each application. A sample of this output for one application is shown in Figure 4.3. The second output saves, on magnetic tape, values of effectiveness, temperature, sliding speed, and actuation force at 21 points for each application (a value of effectiveness at time=0 is not defined). The effectiveness data can then later be analyzed.

Two version of DYNA-DRUM III exist. One is applicable to wedge brakes and the other to cam. Two versions are required because each type of brake uses a different actuating mechanism.

4.7 Comparison of Measured and Calculated Temperatures

It is, of course, important that calculated temperatures correlate well with those that are measured. Comparisons of calculated and measured temperatures for two of the test sequences are shown in Figures 4.4a and b. Because the thermocouple junctions were located about 0.040" below the braking surface, the calculated temperatures in the figures are those for the second node. The second node contains the thermocouple junctions.

ROCKWELL 16-1/2 X 7 S-CAM BRAKE 4PB 693-551D LINING
MVMA PROJECT #1.36 GREENING TESTING LABS TEST M2-13-15 13 JULY,1978
POST-BURNISH EFFECTIVENESS

STOP 8 50 MPH 250 DEG F

	TIME (SEC)	PRESSURE (PSI)	STROKE (IN)	SPEED (MPH)	BRAKE TORQUE (K IN-LBS)	RUBBING SPEED (FPS)	ACTUATION TORQUE (IN-LBS)	TEMPERATURES (DEG F) SURFACE	TO JUNCTION	PERIPHERY	EFFECTIVENESS (IN-LB/IN-LB)
1	0.0	3.8	0.54	51.2	2.7	30.7	0	233	233	233	----
2	0.15	35.1	1.25	50.3	78.3	30.1	5420	283	242	233	14.45
3	0.30	34.3	1.29	48.8	77.4	29.2	5250	324	273	233	14.70
4	0.60	34.0	1.29	46.2	75.6	27.7	5210	369	315	232	14.51
5	0.90	34.3	1.28	43.6	73.2	26.1	5260	395	344	232	13.91
6	1.15	34.0	1.29	41.4	71.7	24.8	5210	410	361	232	13.76
7	1.45	34.3	1.30	38.8	70.3	23.2	5270	422	377	232	13.36
8	1.75	34.0	1.30	36.0	69.3	21.6	5210	431	389	233	13.30
9	2.05	33.9	1.32	33.6	68.8	20.1	5190	437	397	234	13.26
10	2.35	34.1	1.31	31.1	68.7	18.6	5210	441	404	235	13.18
11	2.65	34.3	1.33	28.4	69.4	17.0	5270	443	409	236	12.99
12	2.90	34.0	1.34	26.0	68.1	15.6	5210	443	412	238	13.07
13	3.20	34.0	1.35	23.4	68.1	14.0	5210	442	413	240	13.07
14	3.50	34.0	1.36	21.2	68.7	12.7	5210	440	414	243	13.18
15	3.80	34.0	1.36	18.6	69.6	11.1	5210	437	414	245	13.36
16	4.10	34.0	1.36	16.0	70.2	9.6	5210	433	412	248	13.47
17	4.40	34.5	1.37	13.4	71.1	8.0	5300	428	410	251	13.41
18	4.65	34.5	1.37	11.4	71.8	6.9	5300	423	407	254	13.56
19	4.95	34.5	1.37	8.8	72.7	5.3	5300	416	402	257	13.72
20	5.25	34.5	1.37	5.8	73.5	3.5	5300	407	397	260	13.86
21	5.55	34.5	1.33	2.9	73.8	1.7	5300	396	390	263	13.92
22	5.80	34.5	1.39	0.8	76.2	0.5	5300	387	383	266	14.38

Figure 4.3. Sample page of output from program DYNA-DRUM III.

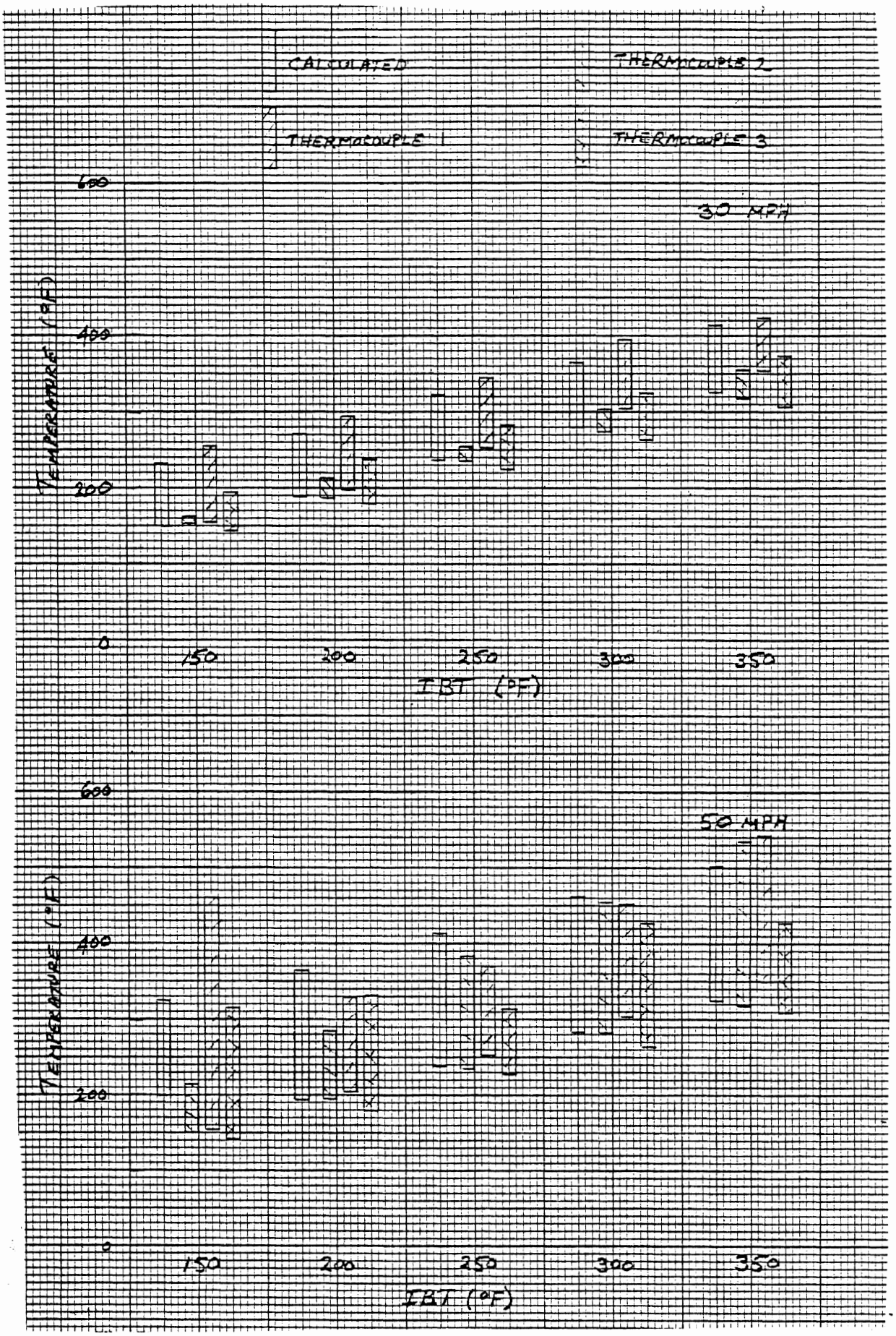

Figure 4.4a. Comparison of calculated and measured temperatures - cam brake with MM8C5 linings - post-burnish effectiveness.

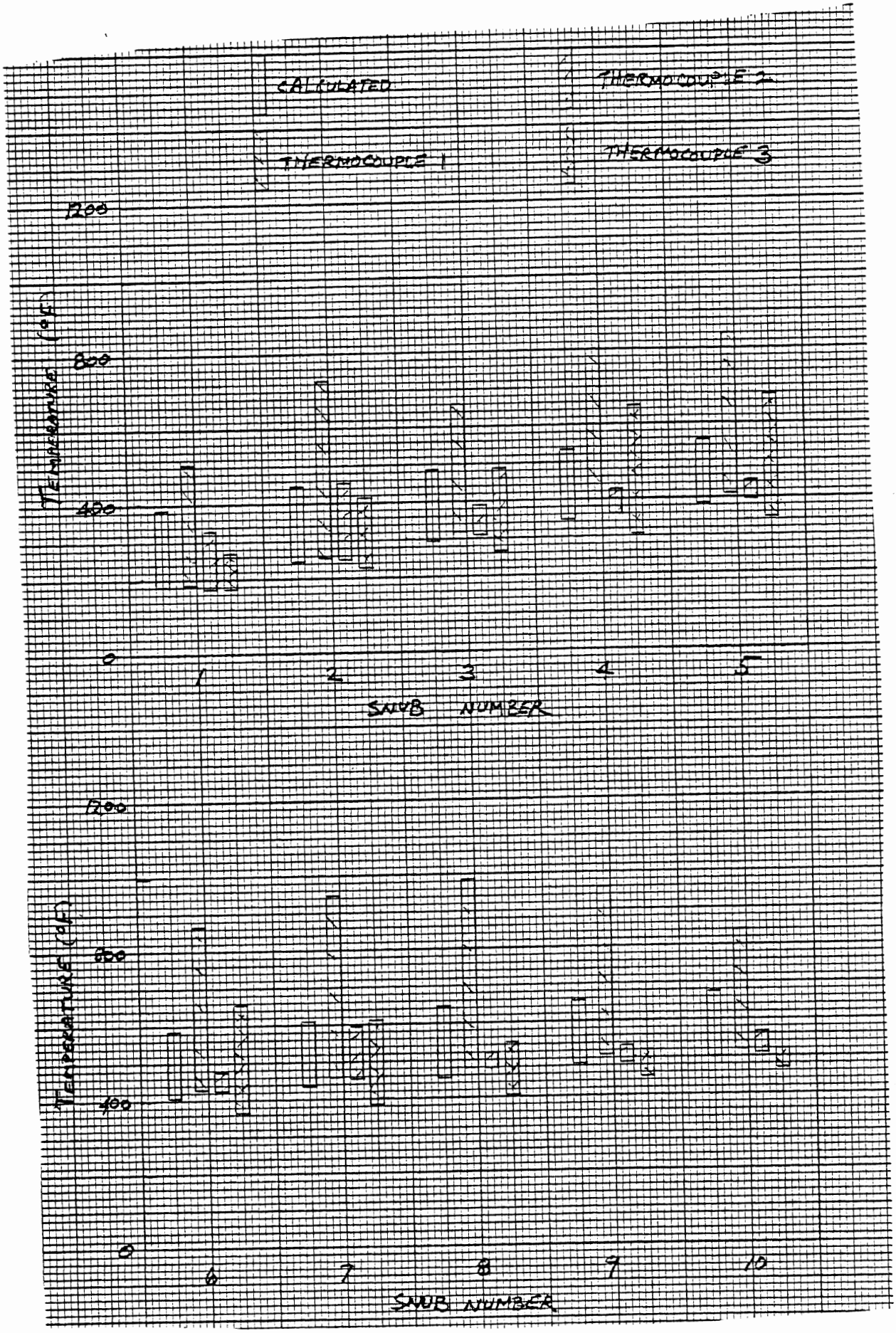

Figure 4.4b. Comparison of calculated and measured temperatures - wedge brake with ABB 693-551D linings - fade.

It is dramatically evident from the figures why measured temperature cannot be used in deriving the effectiveness function. The temperature rises vary considerably across the width of the lining during a brake application. Thus, attempting to measure an average temperature across the width of the lining would be quite difficult, requiring many, many thermocouples or some other very sophisticated measuring scheme. Also, the thermal model shows that the temperature measured by the sub-surface thermocouples lags the temperature at the braking surface. So, even if there was no variation in temperature across the width of the lining, the temperature measured by the sub-surface thermocouples would still have the shortcoming of differing from the temperature at the braking surface. The difference is substantial during the early portion of a brake application.

With the measured temperatures being at such variance with one another, it is difficult to assess how well the calculated temperature matches the average measured temperature over the width of the lining. One can only say that the calculated temperatures appear quite reasonable. Therefore, the validity of the thermal model has been accepted.

4.8 Curve-Fitting the Effectiveness Data

The final step in deriving the effectiveness function is curve-fitting the effectiveness data produced by DYNA-DRUM III. In this study, the data were fitted by a least squares procedure to a multinomial of the following form, viz.:

$$F = \sum_{i=1}^{n_i} \sum_{j=1}^{n_j} \sum_{k=1}^{n_k} a_{ijk}\, \theta^{i-1} v^{j-1} F^{k-1} \qquad (4.6)$$

Note that if two of the independent variables are held constant, the multinomial reduces to a polynomial in the third variable.

Thus, the values of n_i, n_j, and n_k can be guessed by plotting the effectiveness data against one of the independent variables while holding the other two fixed.

The curve fit is performed using a statistical analysis package called MIDAS (Michigan Interactive Data Analysis System) which resides on the Michigan Terminal System, the computer system at The University of Michigan. MIDAS possesses the capability to perform a multi-variable linear least-squares curve fit. Because Equation (4.6) is nonlinear, it must be transformed into a multi-variable linear equation. This is accomplished by expanding the multinomial and making each term of the summation a new independent variable. For example, if the values of n_i, n_j, and n_k are 3, 3, and 3, respectively, the multinomial will consist of 27 terms. Thus, the equation can be expressed as a linear equation with 26 independent variables and one constant term. After the data has undergone this linear transformation, MIDAS can readily calculate the coefficients which provide the least-squares curve fit to Equation (4.6). In addition, MIDAS computes the coefficient of determination, r^2, and the standard error, s_e. These two numerics are also very helpful in determining the values of n_i, n_j, and n_k. The values for these numbers are picked so that the data is adequately described with the simplest equation.

5.0 RESULTS

5.1 Effectiveness Function

Examples of the effectiveness functions which have been calculated from the dynamometer test data are shown graphically in Figures 5.1 and 5.2. (Detailed presentations of all of the effectiveness functions which have been generated are contained in Appendix B.)

Some observations which can be made for the cam brake with ABB 693-551D and MM8C5 linings in the post-burnish condition are:

- effectiveness is most dependent on actuation torque, followed by sliding speed, and then temperature,
- temperature has very little effect, and
- the brake is more effective at high sliding speeds than low sliding speeds.

For the wedge brake with ABB 693-551D and MM8C5 linings during the fade:

- sliding speed has a great influence on effectiveness, as does temperature,
- again, the brake is more effective at high sliding speeds than at low speeds, and
- the MM8C5 lining fades with increasing temperature up to about 500°F, and then begins to get more effective.

Coefficients of determination and standard errors for all of the regressions performed are shown in Table 5.1. The curve fits describe the data very well as is demonstrated by the high values of r^2 and low standard errors. The standard errors are about 3-5% of the average value of effectiveness for each of the regressions,

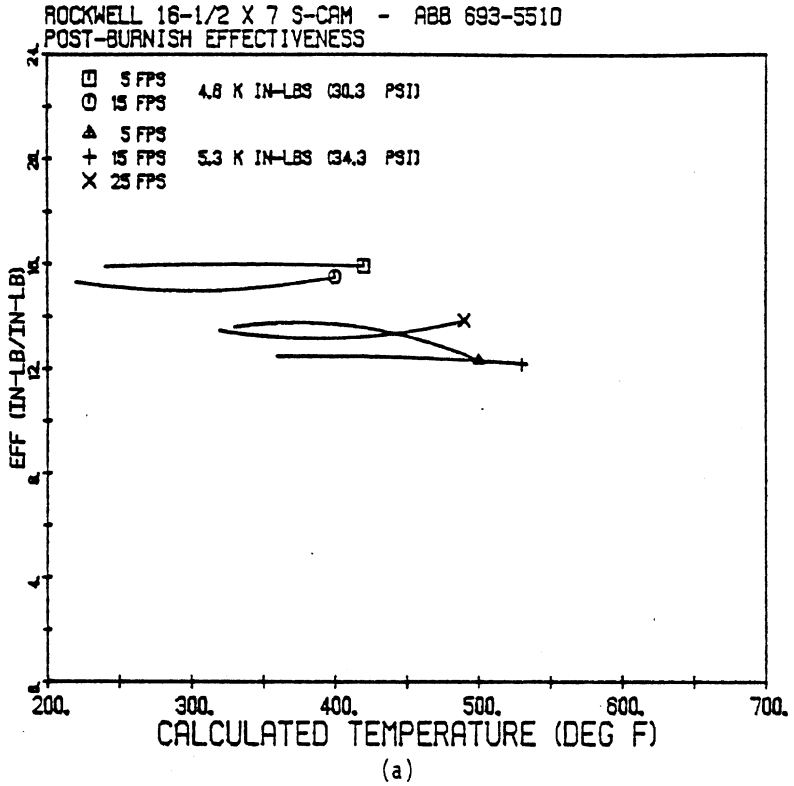

(a)

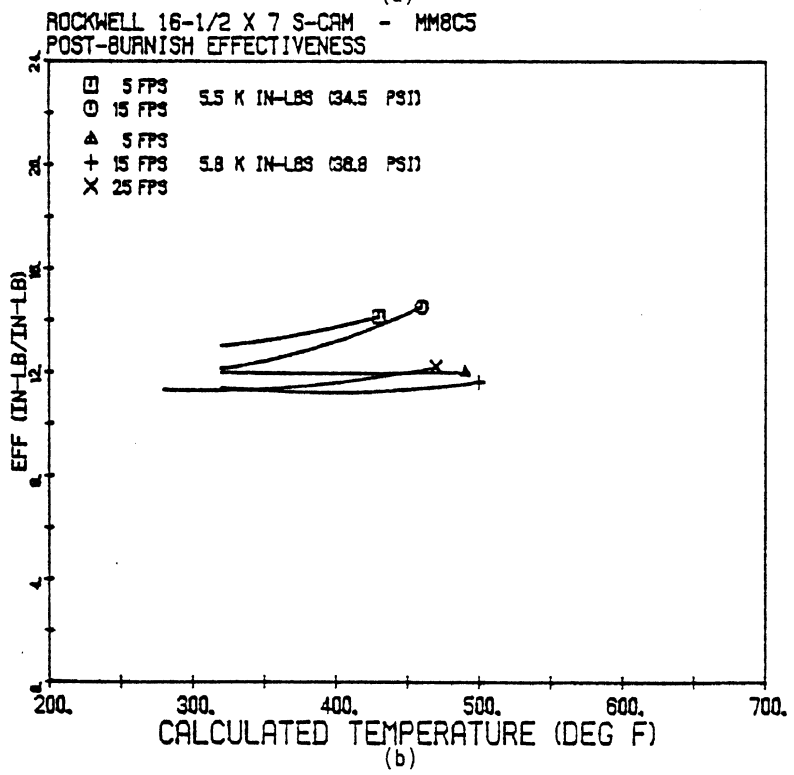

(b)

Figure 5.1. Effectiveness functions for the cam brake with ABB 693-551D and MM8C5 linings - post-burnish effectiveness.

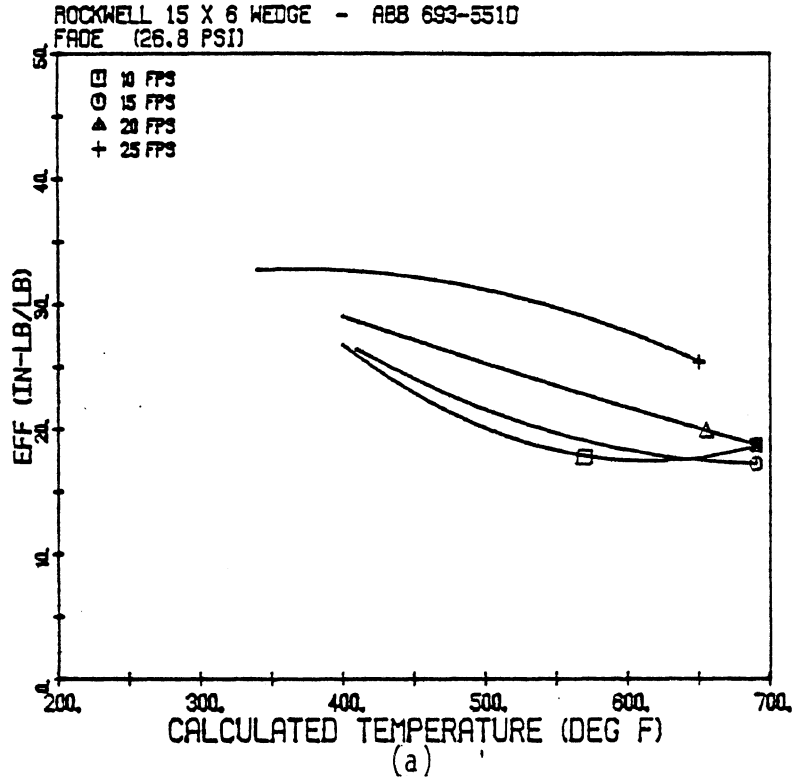

(a)

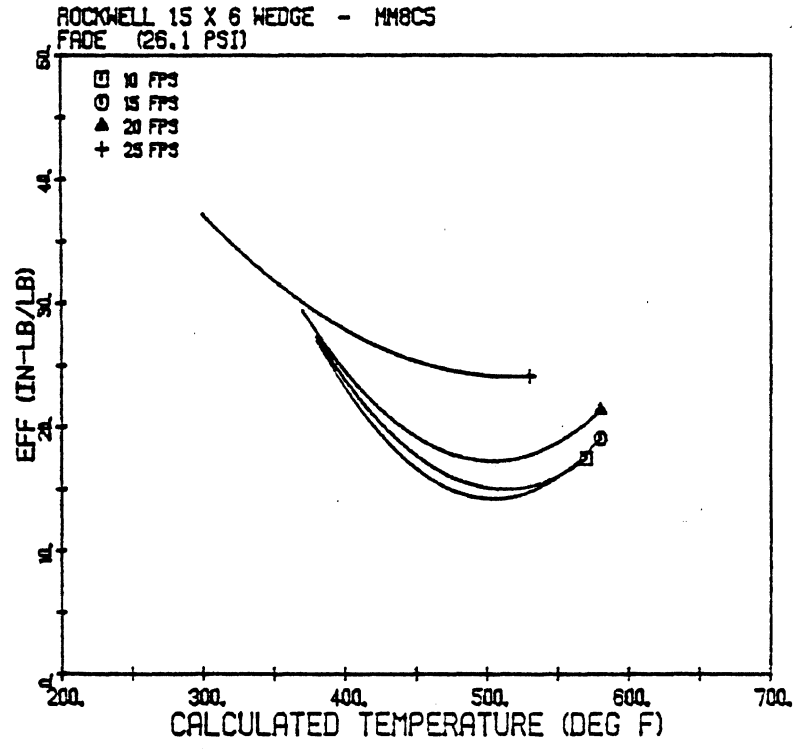

(b)

Figure 5.2. Effectiveness functions for the wedge brake with ABB 693-551D and MM8C5 linings - fade.

Table 5.1. Values of the Coefficient of Determination and Standard Errors for the Regression Analyses.

Brake	Lining		Coefficient of Determination, r^2	Standard Error, S_e
15x6 Wedge	ABB 693-551D	Post-Burnish Eff.	0.980	1.00
		Fade	0.951	1.20
	MM8C5	Post-Burnish Eff.	0.984	0.86
		Fade	0.751	3.02
	E84	Post-Burnish Eff.	0.997	0.58
		Fade	0.937	0.76
16 1/2x7 S-cam	ABB 693-551D	Post-Burnish Eff.	0.951	0.33
		Fade	0.949	0.30
	MM8C5	Post-Burnish Eff.	0.912	0.39
		Fade	0.915	0.42
	E80	Post-Burnish Eff.	0.986	0.21
		Fade	0.927	0.30

which is extremely good. (The regression for the wedge brake fitted with MM8C5 linings for the fade data resulted in a poorer fit than the other regressions. It is suspected that one of the thermocouples was not working properly during this test, so that the temperatures calculated were in error.)

Attempts to regress the recovery data resulted in mixed results. In some cases, the regression was acceptable, in others not. The reason for the lack of success can be seen in Figure 5.3. Here, effectiveness is plotted against stop number at fixed conditions of sliding speed and temperature (actuation force is constant for all of these stops). As can be seen, effectiveness increases as the recovery progresses for about the first seven recovery stops. Thus, there are some rapid changes occurring within the brake during this time which cannot be explained by temperature and sliding speed alone. This behavior is an outstanding example of the effect of work history.

It is very difficult to try to explain with any confidence the mechanism which causes the above phenomenon. However, some reasons can be conjectured. It is thought that during the burnish, two processes occur. The first wears the lining so that it conforms to the curvature of the drum. The second establishes a stable chemical composition of the lining surface. Now, if during the fade, the temperatures occurring at the braking surface get very much higher than they did during the burnish, the lining will become chemically active again and its surface chemistry will change. The amount of this change will depend on reaction rates and phase transformation rates which are in turn dependent on a time at temperature relation. Any changes in the chemical composition of the linings will affect the frictional behavior of the linings. Thus, a fade test can produce a change in the frictional characteristics of the brake. Although this effect is not obvious during the fade, as evidenced by the very successful regression of the effectiveness data, it becomes obvious during the first part of the recovery.

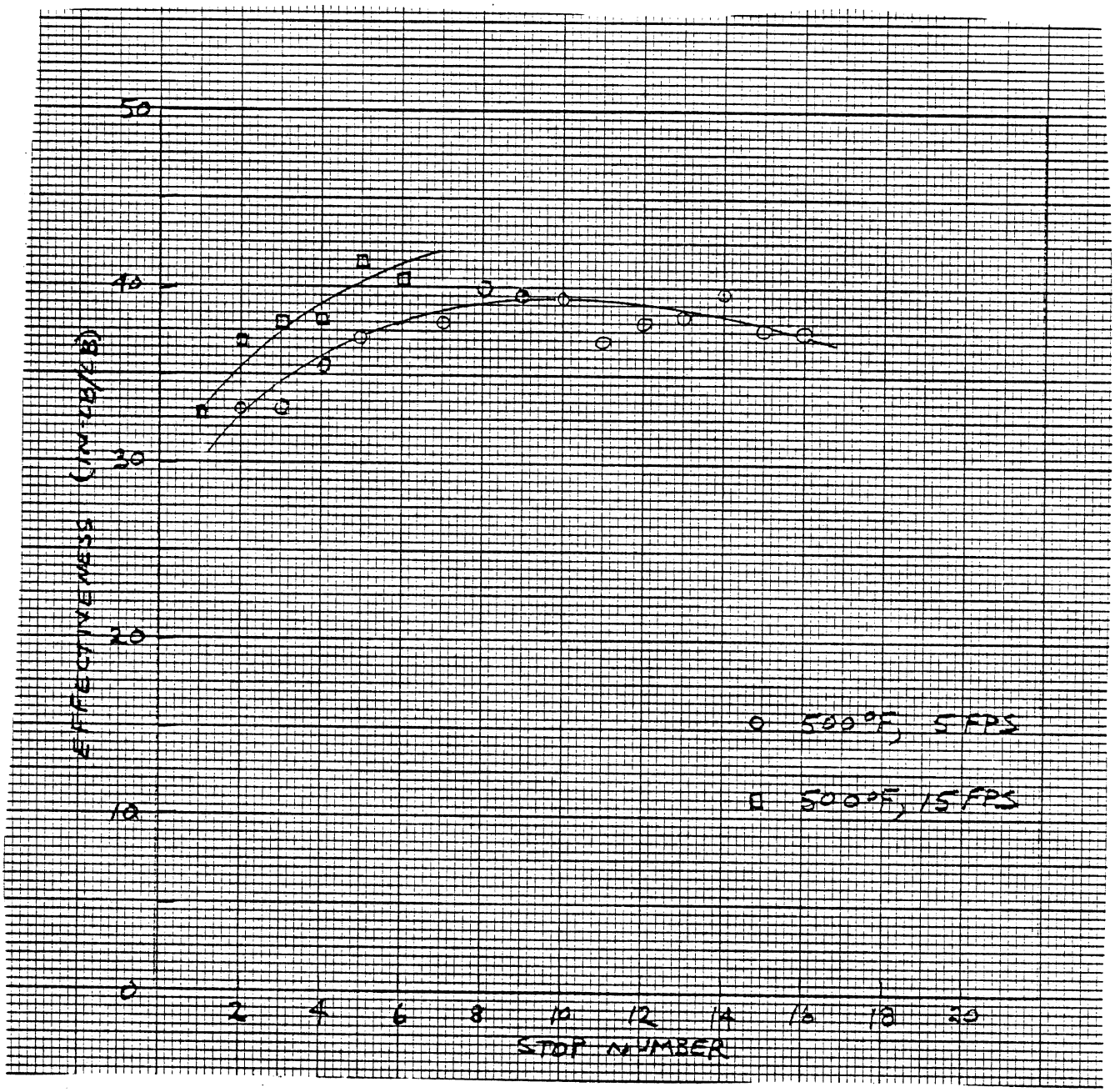

Figure 5.3. Effectiveness vs. stop number during a recovery test - constant temperature and rubbing speed - 15 x 6 wedge - ABB 693-551D.

A second mechanism is mechanical and thermal distortion of the brake drum. Distortion will occur because of temperature gradients existing in the drum. Changes in the pressure distribution across the width of the lining will therefore occur which can change the torque output of the brake. It is conceivable, then, that as the drum is cooling at a fairly rapid rate during the early part of the recovery cycle, the pressure distribution across the lining becomes more favorable and effectiveness is increased.

These two mechanisms point out how sensitive the effectiveness of a brake can be to the rate at which temperatures build during a fade cycle and cool during a recovery cycle. If vehicle test results from a fade and recovery cycle are to be compared with dynamometer results, then the work done by the brake and the time between stops must be quite closely matched between vehicle and dynamometer tests.

5.2 Simulation of Time Histories of Torque

In order to evaluate how well the derived equations can replicate the original time histories generated by the dynamometer tests (from which the equations were derived), a computer program named DRUMSIN was developed. This program uses a time history of actuation force taken from a dynamometer test to calculate a time history of torque. By means of an iterative process, values of interface temperature, rubbing speed, and effectiveness are calculated. Output torque is then simply the product of the actuation force and the computed effectiveness.

Examples of two simulated torque traces are shown in Figures 5.4a and b. The agreement between simulated and measured torque is excellent in both cases. The agreement is especially notable in Figure 5.4a where the torque is far from constant during the stop.

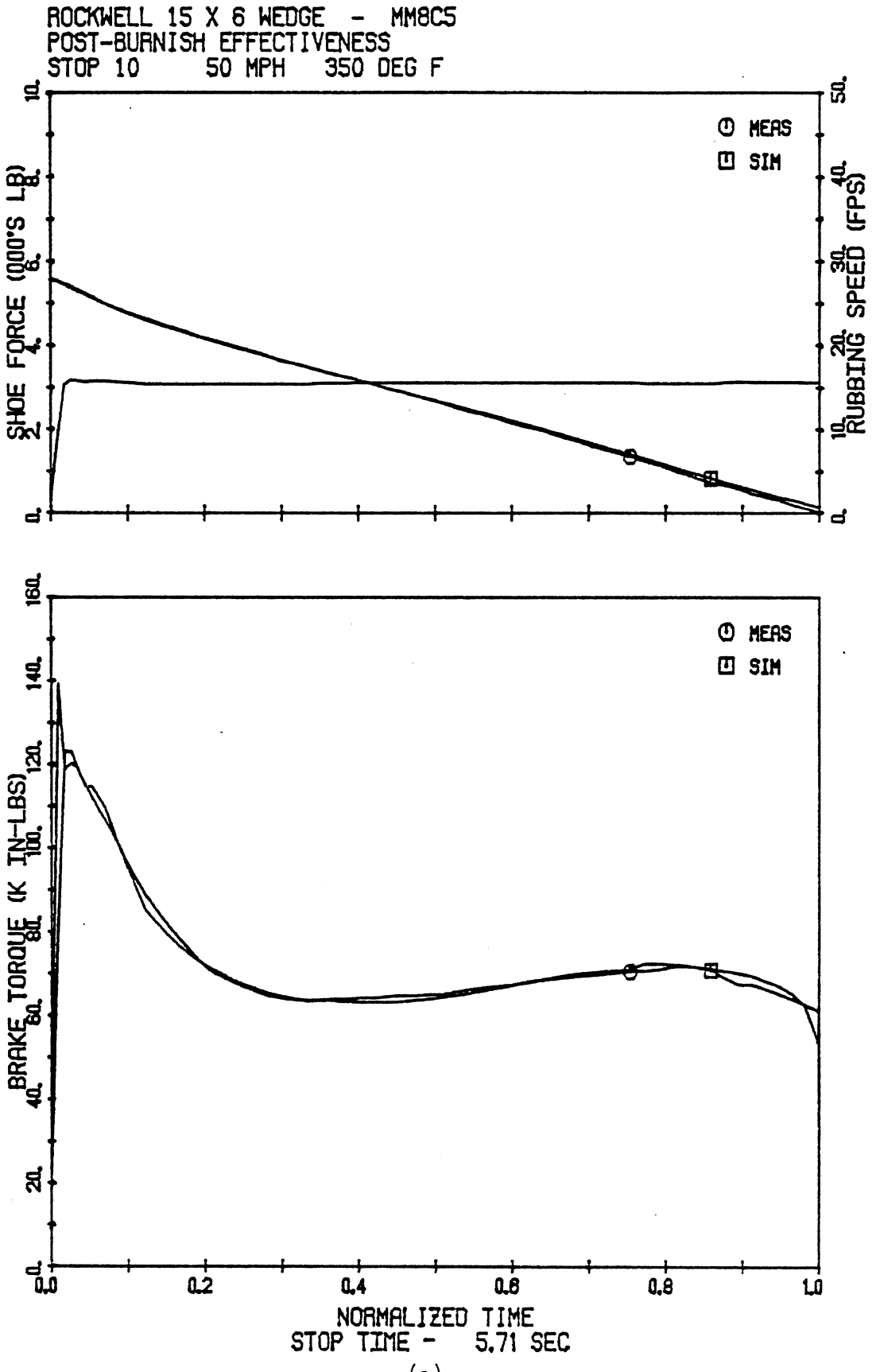

(a)

Figure 5.4. Comparison of simulated and measured time histories of a brake application on the dynamometer.

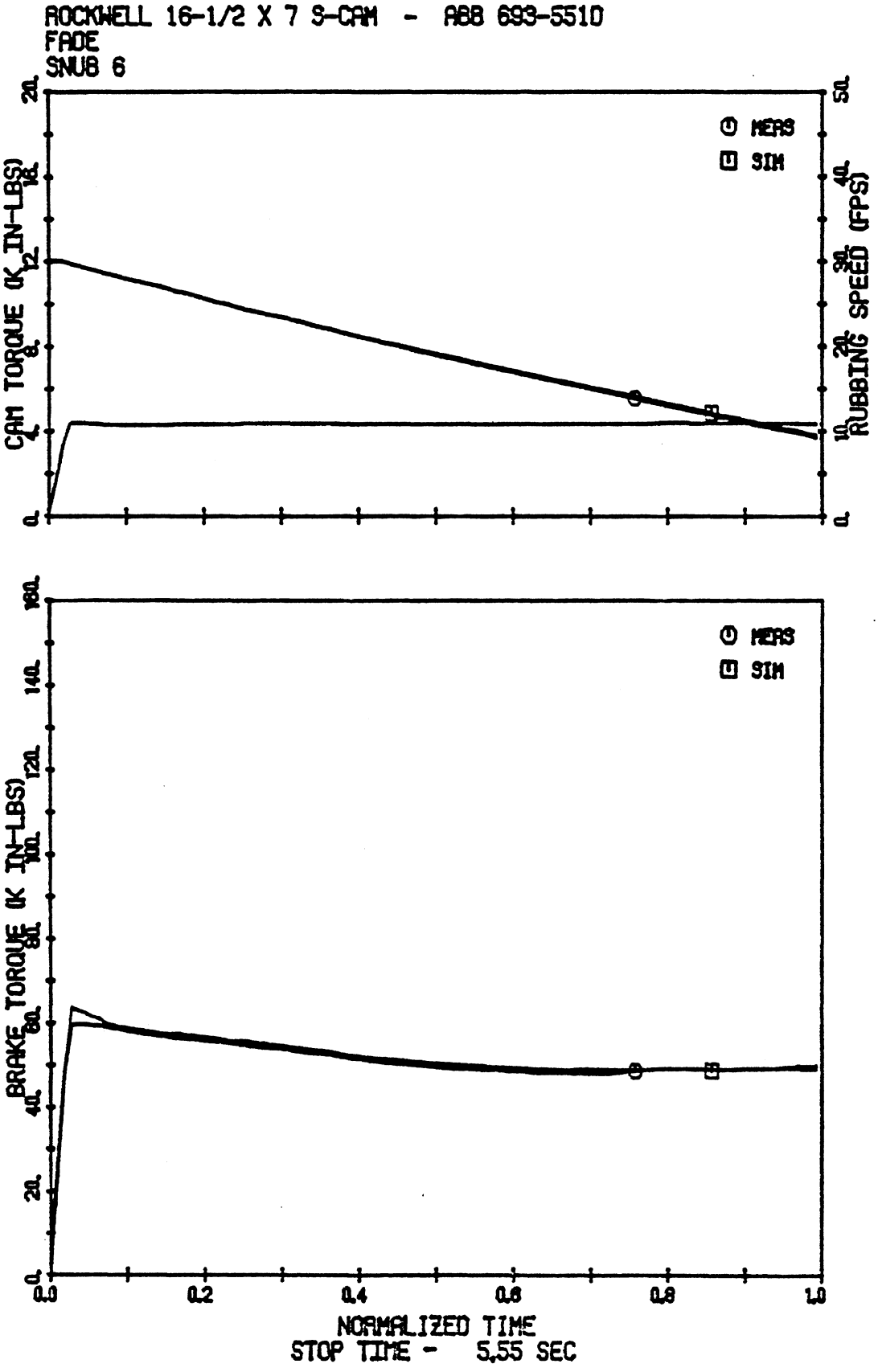

(b)

Figure 5.4. (Cont.)

Torque traces were simulated for a number of other brake applications and showed excellent agreement with measured values.

6.0 EMPLOYING THE BRAKE MODEL IN VEHICLE SIMULATIONS

This section is intended to provide an overview of how the brake model described in Sections 2 through 5 would be incorporated into a large, detailed vehicle simulation such as the one described in Reference [1].

Obviously, a description of the brakes on each axle would be required. This description would consist of: (1) the effectiveness function for the brake/lining combination at each axle for the appropriate work history being simulated; (2) actuation parameters for each brake, that is, air chamber force characteristics and wedge angle or the length of the slack adjuster arm; and (3) parameters describing the finite element model of the brake drum used for computing the interface temperature of each brake.

During each time step of the simulation, a value of torque at each axle would be calculated from the effectiveness function, viz.:

$$T = Fe$$

where

T is torque

F is the actuation force (or torque)

and e is the effectiveness function ($e = e(\theta, v, F)$

(Note that v is equal to wheel speed, ω, multiplied by drum radius, r.) Evaluation of e at each axle would have to be made at each time step. This evaluation would involve a reiterative process in which values of θ, ω, and T at the start of the time step (i.e., from the previous calculation) are used in calculating new values of e, θ, and T at the end of the time step, which is, of course, the start of the next time step.

The value of actuation force, or torque, is available at the beginning of any time step because treadle pressure is an input to the program or, in case an antilock system is used, brake chamber

pressure is determined in another section of the computer program dealing with the antilock system. However, assumptions or calculations concerning stroke in the air chambers at each axle are required to determine actuation force.

Typically, the wheel rotational equations of motion are solved in a separate section of the computer program, thereby providing values of wheel speed, ω, for use in (1) evaluating the effectiveness function, e, and (2) calculating the interface temperature, θ.

A major portion of the brake calculation would be concerned with determining interface temperature. Since the brake model used a calculated interface temperature in its development, it seems wise to use the same temperature calculation method in the overall vehicle simulation. Nevertheless, it is possible that simplified or more computationally efficient means of calculating temperature would be satisfactory as long as they produced results comparable to the finite element model. Computer algorithms with simple, efficient numerical integration methods for solving heat flow problems are available and were used in DRUMSIN.

The following diagram illustrates the information flow proposed for the computation of brake torque, T, at the time $t+\Delta$ based on values of T, ω, and θ evaluated at time t plus F evaluated at $t+\Delta$. (The quantity Δ represents the length of the time step in the digital simulation.) It is of interest to observe that the brake torque calculation uses wheel speed and actuation force as the only input variables.

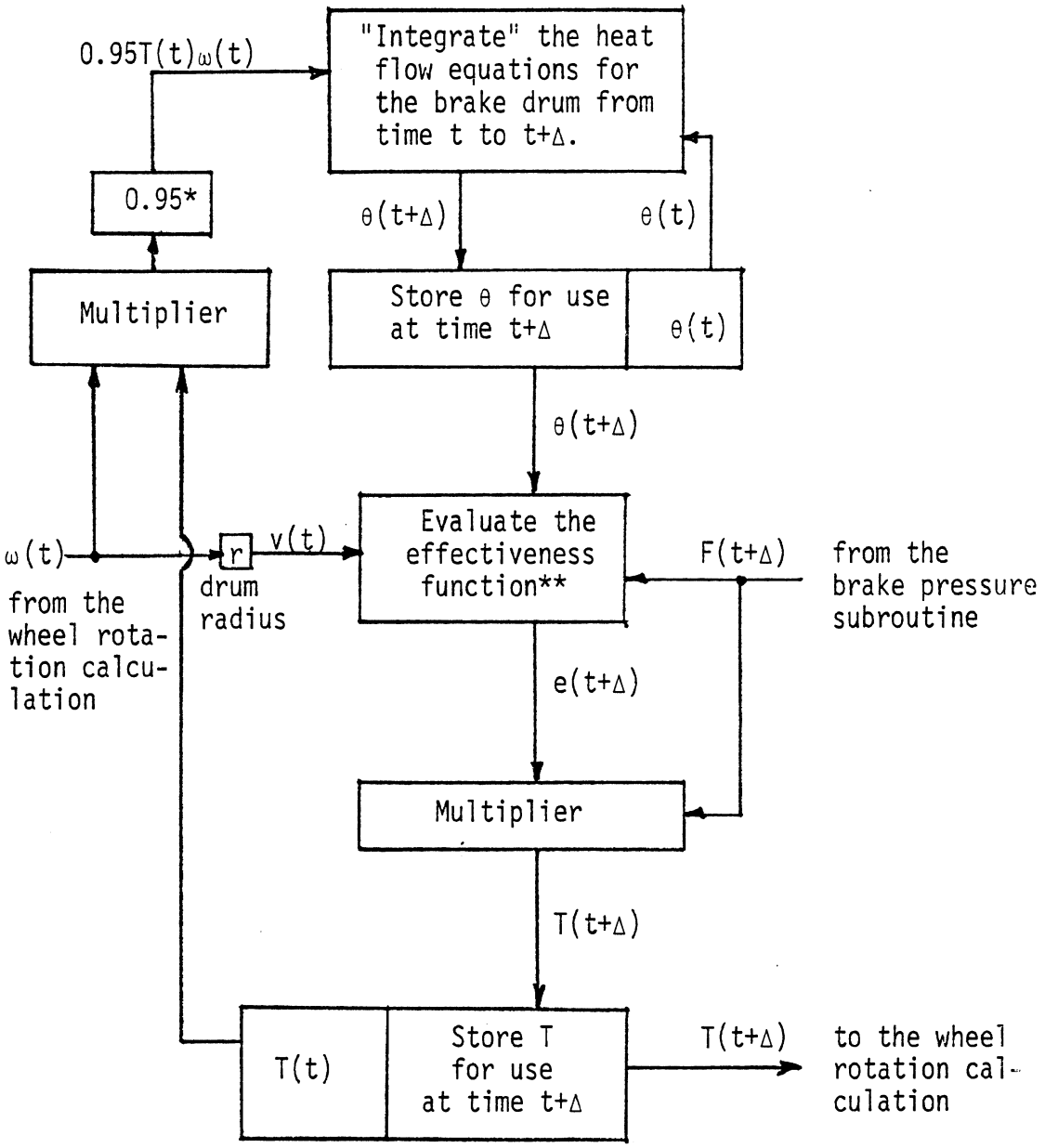

*0.95 is the fraction of total heat flow that goes into the drum.

**Note that this formulation uses the "old" value of wheel speed, $\omega(t)$, to evaluate the "new" value of the effectiveness function, $e(t+\Delta)$.

7.0 CONCLUDING REMARKS - PROPERTIES OF THE BRAKE MODEL AND RECOMMENDATIONS FOR RESEARCH

In summarizing the findings of this study, the following points can be made:

•An empirical model has been developed which treats the mechanical friction brake in a generalized manner. A so-called "black box approach" has been used to identify an effectiveness function which relates brake torque to three independent variables, namely, instantaneous values of actuation force (or torque for cam brakes), sliding velocity, and interface temperature.

•The empirical model provides a valid method for providing a comprehensive representation of torque time histories obtained from dynamometer tests at various initial velocities, initial brake temperatures, and actuation pressure levels (see Section 5.2).

•It should be emphasized that past attempts to organize dynamometer data into tables suitable for predicting braking performance in emergency stops of commercial vehicles has been confounded by (1) the variability of the brake test data available, (2) difficulties in assessing interface temperature, and (3) problems related to work history. The regression analysis method used in this study provides a method for fitting the test data in a manner which furnishes measures of the unaccounted for variability. Sets of data which contain unexpectedly large amounts of unaccounted for variability can be identified.

•The important influence of work history (that is, the previous experience of the brake) is a major problem which affects the interpretation and representation of data from brake tests. In particular, analysis of data obtained during recovery tests indicates unexplained changes in brake torque which are not readily understood on the basis of instantaneous values of sliding speed, interface temperature, and actuation force.

With regard to future research, further work needs to be done on the effects of work history. For example, a post-burnish effectiveness test to characterize a brake for stopping distance performance could be influenced by the order in which various level stops were performed. Special tests which randomize the order in which stops are made are called for to evaluate any work history effect here.

The effects of work history during a fade and recovery sequence could be examined by varying the time between brake applications and/or inertia loading—that is, anything which would influence "time-at-temperature" conditions.

And finally, brake torque variability for one brake and lining needs examining by performing several repeats of a post-burnish effectiveness test. This could also point to certain work history effects which might occur as a brake is repeatedly tested over the same test conditions.

In conclusion, it appears reasonable to attempt to understand and evaluate experimentally the apparent idiosyncracies of pneumatically-actuated brakes using the empirical model developed in this study.

REFERENCES

1. Winkler, C.B., et al., "Predicting the Braking Performance of Trucks and Tractor-Trailers." Highway Safety Research Institute, The University of Michigan, Report No. UM-HSRI-76-26-2, available from NTIS, PB-263216, June 1976.

2. Cook, H.E., et al., "The Development of a Classification Scheme for Brake Linings." Final Report, Contract No. DOT-HS-5-01131, Report No. DOT/HS 802 244/MVSS 105-75, National Highway Traffic Safety Administration, February 1977.

3. Gillespie, T.D., et al., "Modeling the In-Stop Torque Performance of Hydraulic Truck Brakes." Highway Safety Research Institute, The University of Michigan, Report No. UM-HSRI-78-58, December 1978.

4. Newcomb and Spurr, Braking of Road Vehicles. Chapman and Hall, Ltd., London, 1967.

5. Rusnak, R.M., et al., "A Comparison by Thermal Analysis of Rotor Alloys for Automobile Disc Brakes." SAE Paper No. 700137, 1970.

6. Rhee, S.K., et al., "An Inertial Dynamometer Evaluation of Three Alloys for Automotive Brake Drums." SAE Paper No. 700138, 1970.

APPENDIX A

INERTIAL DYNAMOMETER TEST PROCEDURE

1. Test Set-Up

1.1 Ambient temperature

The ambient temperature shall be between 75°F and 100°F

1.2 Cooling air

Air at ambient temperature shall be directed continuously and uniformly over the brake at a speed of 2200 fpm.

1.3 Instrumentation

Instrumentation shall be provided to autographically record the following data:

a) line pressure
b) brake torque
c) dynamometer shaft speed
d) lining temperature
e) temperature at braking surface of drum at three points
f) temperature of periphery of drum in line with the center of the braking surface

1.4 Wheel load

The wheel load is 9,000 lb.

1.5 Tire radius

The tire radius is 20.2 in.

1.6 Dynamometer speed

The shaft speed of the dynamometer is given by the relation $\text{rpm} = 8.32\ V$
where V denotes vehicle speed in mph.

1.7 Dynamometer inertia

The dynamometer inertia is 793 ± 5% slug-ft^2

2. Test Notes

2.1 Initial brake temperature (IBT) is defined as the lining temperature at the time of brake application.

2.2 Specified decelerations are the average value computed from the time of onset of deceleration to the time of completion of the stop or snub.

2.3 The specified line pressures shall be attained in not more than 0.30 sec.

2.4 The brake temperature may be raised to a specified level by making one or more stops from 40 mph at a deceleration of 10 fpsps. The brake temperature may be lowered to a specified level by rotating the drum at 30 mph.

2.5 Tolerances on the test variables are as follows:

a) dynamometer speed - ±2 mph
b) line pressure - ±2 psi
c) deceleration - ±1 fpsps
d) initial brake temperature - ±10°F

3. Test Procedure

3.1 Instrumentation check stops

Adjust brake. Make 10 stops from 30 mph at a line pressure of 30 psi. Correct any malfunctions which occur.

3.2 Burnish

Make 200 stops from 40 mph at a deceleration of 10 fpsps. Initial brake temperature shall not be less than 315°F nor greater than 385°F. Make 200 additional stops with an IBT of not less than 450°F nor greater than 550°F. Adjust brake. Record first and last stops in each temperature series as well as each twentieth stop in each series.

3.3 Post-burnish effectiveness

Establish the line pressures required to generate a deceleration of 12 fpsps from both 30 mph and 50 mph with an IBT of 150°F, but do not exceed 80 psi. Make

five stops from 30 mph at the previously-determined line pressure at IBT's of 150, 200, 250, 300, and 350°F. Then, make five stops from 50 mph using the line pressure determined above at IBT's of 150, 200, 250, 300, and 350°F. Record all stops.

3.4 Fade and recovery

Establish the line pressures required to yield decelerations of 10 fpsps during a snub from 50 mph to 15 mph, 12 fpsps during a stop from 30 mph, and 14 fpsps during a stop from 20 mph with an IBT of 175°F, but do not exceed 80 psi.

Make 10 snubs from 50 mph to 15 mph at the pressure determined above. The initial brake temperature for the first stop is 175°F. Make stops at intervals of 72 seconds measured between the starts of successive stops.

One minute after completion of the tenth stop, make one stop from 20 mph at the pressure determined previously.

Two minutes after the previous stop, begin a series of 20 stops from 30 mph at the previously-determined pressure. The interval between starts of successive stops is one minute.

Record all stops.

APPENDIX B

EFFECTIVENESS FUNCTIONS

This appendix contains detailed presentations of the effectiveness functions obtained for each brake. The effectiveness functions for the post-burnish effectiveness are of the following form:

$$e = \sum_{i=1}^{n_i} \sum_{j=1}^{n_j} \sum_{k=1}^{n_k} a_{ijk}\, \theta^{i-1} v^{j-1} F^{k-1}$$

where

- e = effectiveness (in-lb/lb for wedge brake; in-lb/in-lb for cam brake)
- θ = interface temperature (°F)
- v = sliding speed (fps)
- F = actuation force/torque (lbs for wedge brake; in-lbs for cam brake)

For the fade, they are of the form:

$$e = \sum_{i=1}^{n_i} \sum_{j=1}^{n_j} a_{ij}\, \theta^{i-1} v^{j-1}$$

The format of each presentation for each brake/lining combination is as follows:

1) designation of brake and lining
2) post-burnish effectiveness function
   - i) values of n_i, n_j, and n_k
   - ii) coefficients a_{ijk}
   - iii) description of the bounds on the effectiveness function

3) fade effectiveness function

   i) values of n_i and n_j

   ii) coefficients a_{ij}

   iii) description of bounds on effectiveness function

4) graphical presentation of effectiveness functions

BRAKE: 15 x 6 Wedge

LINING: ABB 693-551D

POST-BURNISH EFFECTIVENESS

		$n_i = 3$	$n_j = 4$	$n_k = 2$
$n_k = 1$	$n_i =$	1	2	3
$n_j = 1$		86.095	-57.506×10^{-3}	48.439×10^{-6}
2		-4.8803	37.509×10^{-3}	-73.350×10^{-6}
3		1.7263	-10.412×10^{-3}	15.448×10^{-6}
4		-0.061661	0.37315×10^{-3}	-0.52920×10^{-6}
$n_k = 2$				
	$n_i =$	1	2	3
$n_j = 1$		-29.356×10^{-3}	54.649×10^{-6}	-64.169×10^{-9}
2		-1.9979×10^{-3}	4.2873×10^{-6}	7.4656×10^{-9}
3		-0.37225×10^{-3}	2.4195×10^{-6}	-3.9813×10^{-9}
4		0.017981×10^{-3}	-0.10735×10^{-6}	0.15498×10^{-9}

Bounds

Actuation Force: 1900 lbs $\leq F \leq$ 2900 lbs

Sliding Speed: Lower v = 0 fps
Upper missing

Interface Temperature:

Lower $\theta = 21.841 + 38.453v - 4.3639v^2 + 0.076874v^3 + 0.11292F - 0.013242vF + 1.7944 \times 10^{-3}v^2F - 0.039306 \times 10^{-3}v^3F$

Upper $\theta = 177.06 + 50.613v - 6.9024v^2 + 0.18223v^3 + 0.12349F - 0.016661vF + 2.6490 \times 10^{-3}v^2F - 0.075605v^3F$

FADE

$n_i = 3 \quad n_j = 3$

n_j \ n_i	1	2	3
1	137.10	-416.86×10^{-3}	379.99×10^{-6}
2	-3.9849	14.598×10^{-3}	-16.484×10^{-6}
3	-0.027173	0.19055×10^{-3}	-0.095732×10^{-6}

Bounds

Actuation Force: F = 2040 lbs

Sliding Speed: 8.4 fps $\leq$ v $\leq$ 27.2 fps

Interface Temperature:

Lower $\theta = 507.73 - 29.069v + 2.4788v^2 - 0.063904v^3$

Upper $\theta = 816.20 - 31.078v + 2.3994v^2 - 0.057517v^3$

BRAKE: 15 x 6 Wedge

LINING: MM8C5

POST-BURNISH EFFECTIVENESS

$n_i = 3 \quad n_j = 4 \quad n_k = 2$

$n_k = 1$

n_j \ n_i =	1	2	3
1	49.415	40.330×10^{-3}	10.003×10^{-6}
2	24.421	-156.00×10^{-3}	223.68×10^{-6}
3	-4.5730	26.623×10^{-3}	-35.237×10^{-6}
4	0.18421	-0.92392×10^{-3}	1.0809×10^{-6}

$n_k = 2$

n_j \ n_i =	1	2	3
1	-11.115×10^{-3}	-0.60695×10^{-6}	-23.065×10^{-9}
2	-7.6114×10^{-3}	49.130×10^{-6}	-68.598×10^{-9}
3	1.3532×10^{-3}	-8.2393×10^{-6}	10.882×10^{-9}
4	-0.055236×10^{-3}	0.28708×10^{-6}	-0.33490×10^{-9}

Bounds

Actuation Force: 2200 lbs $\leq F \leq$ 3100 lbs

Sliding Speed: Lower $v = 0$ fps

Upper $v = -9.1292 + 0.011563F$

Interface Temperature:

Lower $\theta = -77.632 + 52.410v - 6.3180v^2 + 0.14026v^3$
$+0.13541F - 0.017451vF + 2.3302 \times 10^{-3}v^2F$
$- 0.056445 \times 10^{-3}v^3F$

Upper $\theta = 86.796 + 48.912v - 5.2589v^2 + 0.064536v^3$
$+ 0.13481F - 0.015991vF + 2.0068 \times 10^{-3}v^2F$
$- 0.033511 \times 10^{-3}v^3F$

FADE

$n_i = 3 \quad n_j = 3$

n_j \ n_i	1	2	3
1	-22.535	262.87×10^{-3}	-321.95×10^{-6}
2	34.229	-151.23×10^{-3}	157.09×10^{-6}
3	-1.1754	5.1666×10^{-3}	-5.3209×10^{-6}

Bounds

Actuation Force: $F = 1940$ lbs

Sliding Speed: $8.2 \text{ fps} \leq v \leq 27.1 \text{ fps}$

Interface Temperature:

Lower $\theta = 554.27 - 42.672v + 3.2781v^2 - 0.079383v^3$

Upper $\theta = 721.32 - 38.151v + 3.0121v^2 - 0.072265v^3$

BRAKE: 15 x 6 Wedge

LINING: E84

POST-BURNISH EFFECTIVENESS

$n_i = 3 \quad n_j = 4 \quad n_k = 2$

$n_k = 1$

n_j \ n_i	1	2	3
1	66.821	0.090638×10^{-3}	-195.22×10^{-6}
2	-27.086	148.57×10^{-3}	-184.68×10^{-6}
3	3.5442	-19.629×10^{-3}	24.968×10^{-6}
4	-0.11816	0.65213×10^{-3}	-0.82366×10^{-6}

$n_k = 2$

n_j \ n_i	1	2	3
1	-22.195×10^{-3}	58.781×10^{-6}	-35.655×10^{-9}
2	4.2519×10^{-3}	-26.321×10^{-6}	35.209×10^{-9}
3	-0.62167×10^{-3}	3.6048×10^{-6}	-4.7479×10^{-9}
4	0.023001×10^{-3}	-0.12803×10^{-6}	0.16368×10^{-9}

Bounds

Actuation Force: $2500 \text{ lbs} \leq F \leq 4400 \text{ lbs}$

Sliding Speed: Lower $v = 0$ fps

Upper $v = 2.7941 + 5.4741 \times 10^{-3}F$

Interface Temperature:

Lower $\theta = 100.88 + 23.554v - 1.7407v^2 - 0.017312v^3 + 0.054980F - 5.7896 \times 10^{-3}vF + 0.58408 \times 10^{-3}v^2F - 3.3088 \times 10^{-6}v^3F$

Upper $\theta = 296.94 + 16.745v - 1.1100v^2 - 0.027729v^3 + 0.045276F - 3.8348 \times 10^{-3}vF + 0.40654 \times 10^{-3}v^2F - 0.15175 \times 10^{-6}v^3F$

FADE

$n_i = 3 \quad n_j = 4$

n_j =	n_i = 1	2	3
1	269.99	-904.21×10^{-3}	769.98×10^{-6}
2	-54.235	193.80×10^{-3}	-170.97×10^{-6}
3	3.8772	-14.104×10^{-3}	12.611×10^{-6}
4	-0.079010	0.28901×10^{-3}	-0.25851×10^{-6}

Bounds

Actuation Force: F = 3820 lbs

Sliding Speed: $8.3 \text{ fps} \leq v \leq 27.4 \text{ fps}$

Interface Temperature:

Lower $\theta = 608.43 - 51.824v + 3.8026v^2 - 0.086479v^3$

Upper $\theta = 700.88 - 21.521v + 1.9087v^2 - 0.049422v^3$

BRAKE: 16 1/2 x 7 S-cam

LINING: ABB 693-551D

POST-BURNISH EFFECTIVENESS

$n_i = 3 \quad n_j = 4 \quad n_k = 2$

$n_k = 1$

n_j \ n_i	1	2	3
1	-18.908	247.96×10^{-3}	-276.44×10^{-6}
2	36.868	-187.80×10^{-3}	227.22×10^{-6}
3	-2.7007	13.355×10^{-3}	-15.328×10^{-6}
4	0.045555	-0.21958×10^{-3}	0.23707×10^{-6}

$n_k = 2$

n_j \ n_i	1	2	3
1	6.0432×10^{-3}	-42.464×10^{-6}	42.024×10^{-9}
2	-7.7275×10^{-3}	38.549×10^{-6}	-45.726×10^{-9}
3	0.58130×10^{-3}	-2.8423×10^{-6}	3.2235×10^{-9}
4	-0.010112×10^{-3}	0.048458×10^{-6}	-0.051982×10^{-9}

Bounds

Actuation Torque: $4600 \text{ in-lbs} \leq F \leq 5300 \text{ in-lbs}$

Sliding Speed: Lower $v = 0$ fps

Upper $v = -18.580 + 8.9819 \times 10^{-3} F$

Interface Temperature:

Lower $\theta = -528.88 + 94.808v - 13.474v^2 + 0.43882v^3 + 0.15776F - 0.017088vF + 2.5543 \times 10^{-3}v^2F - 0.084440 \times 10^{-3}v^3F$

Upper $\theta = -222.81 + 78.964v - 12.136v^2 + 0.39732v^3 + 0.13193F - 0.014139vF + 2.3166 \times 10^{-3}v^2F - 0.077037 \times 10^{-3}v^3F$

FADE

$n_i = 4 \quad n_j = 3$

n_j \ n_i	1	2	3	4
1	-87.103	693.65×10^{-3}	-1513.0×10^{-6}	1052.8×10^{-9}
2	4.6168	-34.243×10^{-3}	77.497×10^{-6}	-56.608×10^{-9}
3	-0.042488	0.40049×10^{-3}	-1.0037×10^{-6}	0.80831×10^{-9}

Bounds

Actuation Torque: F = 4360 in-lbs

Sliding Speed: $9.3 \text{ fps} \leq v \leq 30.0 \text{ fps}$

Interface Temperature:

Lower $\theta = 516.09 - 34.284v + 2.3237v^2 - 0.050372v^3$

Upper $\theta = 707.20 - 25.992v + 1.8986v^2 - 0.042721v^3$

BRAKE: 16 1/2 x 7 S-cam

LINING: MM8C5

POST-BURNISH EFFECTIVENESS

$n_i = 3 \quad n_j = 4 \quad n_k = 2$

$n_k = 1$

n_j \ n_i	1	2	3
1	277.48	-1430.2×10^{-3}	2193.6×10^{-6}
2	-66.559	352.25×10^{-3}	-485.92×10^{-6}
3	4.5933	-25.751×10^{-3}	37.760×10^{-6}
4	-0.090714	0.53506×10^{-3}	-0.83060×10^{-6}

$n_k = 2$

n_j \ n_i	1	2	3
1	-46.476×10^{-3}	249.97×10^{-6}	-382.37×10^{-9}
2	11.688×10^{-3}	-61.721×10^{-6}	84.994×10^{-9}
3	-0.80160×10^{-3}	4.4711×10^{-6}	-6.5498×10^{-9}
4	0.015716×10^{-3}	-0.092358×10^{-6}	0.14347×10^{-9}

Bounds

Actuation Torque: $5500 \text{ in-lbs} \leq F \leq 5800 \text{ in-lbs}$

Sliding Speed: Lower $v = 0$ fps

Upper $v = -15.188 + 8.0468 \times 10^{-3}F$

Interface Temperature:

Lower $\theta = -1089.7 - 53.085v + 8.9186v^2 - 0.22660v^3 + 0.24346F + 9.1749 \times 10^{-3}vF - 1.5275 \times 10^{-3}v^2F + 0.038158 \times 10^{-3}v^3F$

Upper $\theta = -206.16 - 176.17v + 16.020v^2 - 0.34450v^3 + 0.11751F + 0.030882vF - 2.7590 \times 10^{-3}v^2F + 0.058348 \times 10^{-3}v^3F$

FADE

$n_i = 4 \quad n_j = 3$

n_j \ n_i	1	2	3	4
1	63.096	-339.61×10^{-3}	763.51×10^{-6}	-553.48×10^{-9}
2	-16.164	113.13×10^{-3}	-260.82×10^{-6}	192.46×10^{-9}
3	0.47102	-3.3114×10^{-3}	7.6611×10^{-6}	-5.6583×10^{-9}

Bounds

Actuation Torque: F = 4800 in-lbs

Sliding Speed: $9.3 \text{ fps} \leq v \leq 30.3 \text{ fps}$

Interface Temperature:

Lower $\theta = 451.07 - 22.497v + 1.6385v^2 - 0.037834v^3$

Upper $\theta = 739.17 - 28.021v + 1.9633v^2 - 0.042949v^3$

BRAKE: 16 1/2 x 7 S-cam

LINING: E80

POST-BURNISH EFFECTIVENESS

$n_i = 3 \quad n_j = 4 \quad n_k = 2$

$n_k = 1$

n_j \ n_i	1	2	3
1	22.351	-49.722×10^{-3}	75.962×10^{-6}
2	-12.886	82.108×10^{-3}	-123.25×10^{-6}
3	1.2319	-8.3162×10^{-3}	12.831×10^{-6}
4	-0.031928	0.21985×10^{-3}	-0.34722×10^{-6}

$n_k = 2$

n_j \ n_i	1	2	3
1	-0.24734×10^{-3}	-1.3089×10^{-6}	-1.0202×10^{-9}
2	1.4361×10^{-3}	-9.1871×10^{-6}	13.745×10^{-9}
3	-0.13853×10^{-3}	0.94308×10^{-6}	-1.4532×10^{-9}
4	3.35562×10^{-3}	-0.024780×10^{-6}	0.039099×10^{-9}

Bounds

Actuation Torque: $7100 \text{ in-lbs} \leq F \leq 9400 \text{ in-lbs}$

Sliding Speed: Lower $v = 0$ fps

Upper $v = -3.1815 + 3.4741 \times 10^{-3}F$

Interface Temperature:

Lower $\theta = -28.063 + 17.719v - 2.3759v^2 + 0.041770v^3 + 0.034759F - 1.6520 \times 10^{-3}vF + 0.28882 \times 10^{-3}v^2F - 6.2330 \times 10^{-6}v^3F$

Upper $\theta = 188.68 + 23.287v - 2.9367v^2 + 0.063696v^3 + 0.028895F - 2.2759 \times 10^{-3}vF + 0.34011 \times 10^{-3}v^2F - 8.2651 \times 10^{-6}v^3F$

FADE

$n_i = 4 \quad n_j = 4$

n_j \ n_i	1	2	3	4
1	-322.84	2191.6×10^{-3}	-4675.8×10^{-6}	3228.1×10^{-9}
2	67.036	-442.63×10^{-3}	937.02×10^{-6}	-642.98×10^{-9}
3	-3.2330	21.592×10^{-3}	-45.916×10^{-6}	31.487×10^{-9}
4	0.045824	-0.31048×10^{-3}	0.66248×10^{-6}	-0.45260×10^{-9}

Bounds

Actuation Torque: 7610 in-lbs

Sliding Speed: $9.2 \text{ fps} \leq v \leq 30.2 \text{ fps}$

Interface Temperature:

Lower $\theta = 456.99 - 25.208v + 1.8790v^2 - 0.043370v^3$

Upper $\theta = 635.01 - 14.004v + 0.99238v^2 - 0.023707v^3$

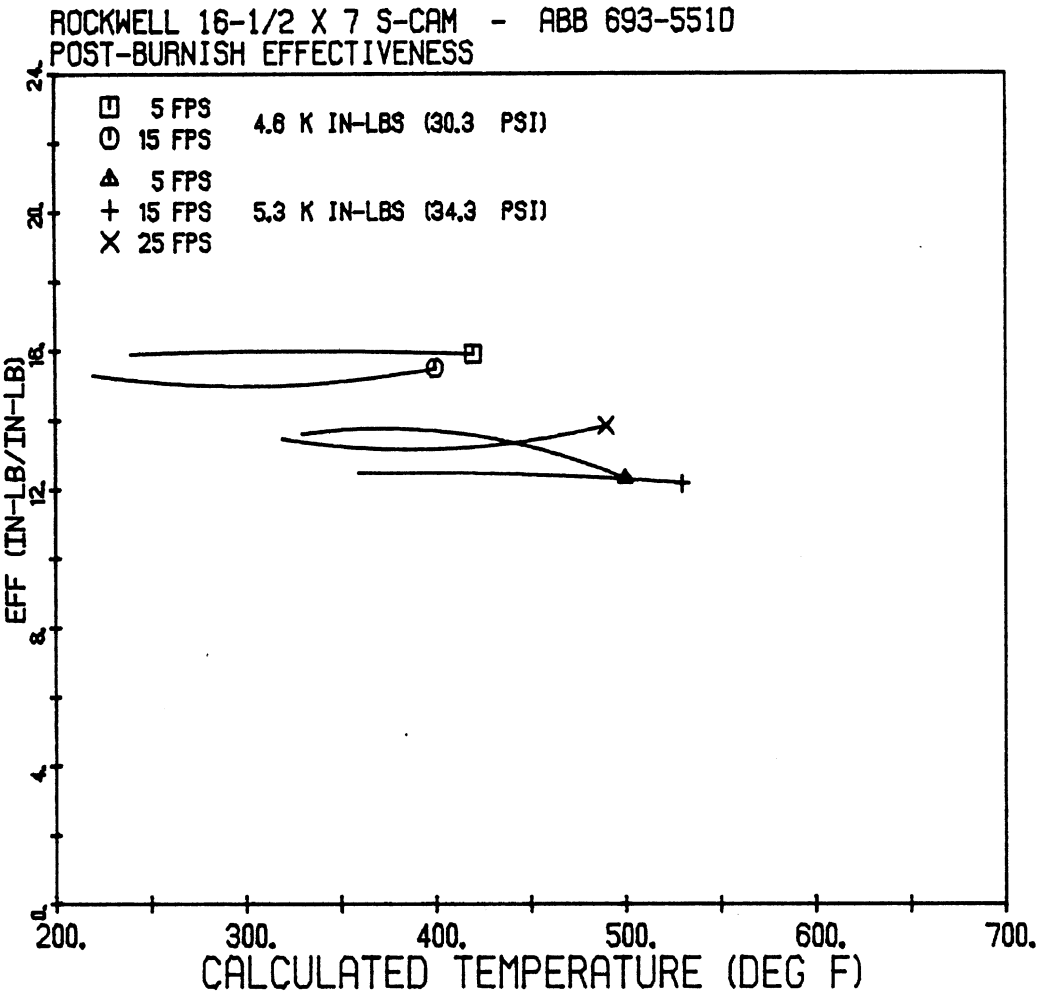
ROCKWELL 16-1/2 X 7 S-CAM - ABB 693-551D
POST-BURNISH EFFECTIVENESS
5 FPS
15 FPS
4.6 K IN-LBS (30.3 PSI)
5 FPS
15 FPS
25 FPS
5.3 K IN-LBS (34.3 PSI)
EFF (IN-LB/IN-LB)
0.
4.
8.
12.
16.
20.
24.
200.
300.
400.
500.
600.
700.
CALCULATED TEMPERATURE (DEG F)

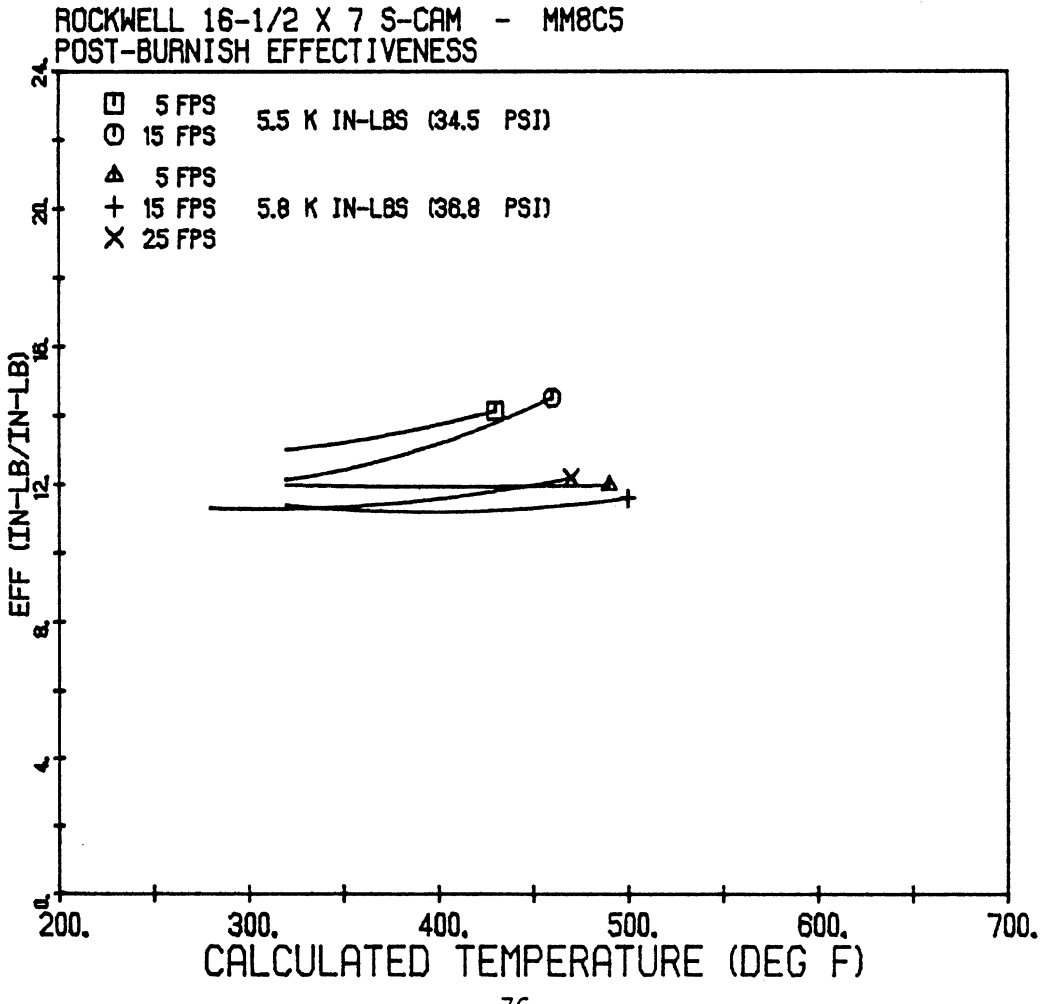
ROCKWELL 16-1/2 X 7 S-CAM - MM8C5
POST-BURNISH EFFECTIVENESS
5 FPS
15 FPS
5.5 K IN-LBS (34.5 PSI)
5 FPS
15 FPS
25 FPS
5.8 K IN-LBS (36.8 PSI)
EFF (IN-LB/IN-LB)
0.
4.
8.
12.
16.
20.
24.
200.
300.
400.
500.
600.
700.
CALCULATED TEMPERATURE (DEG F)

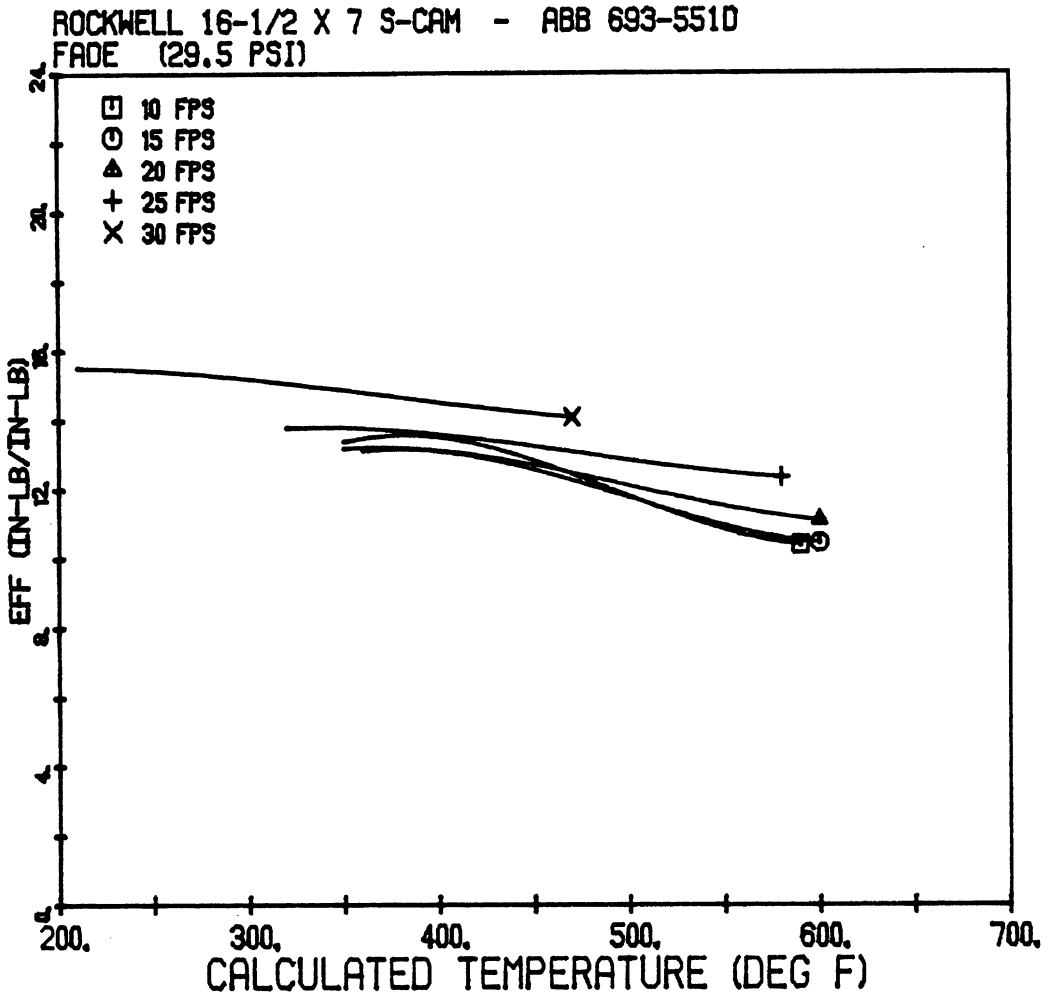
ROCKWELL 16-1/2 X 7 S-CAM - ABB 693-551D
FADE (29.5 PSI)
10 FPS
15 FPS
20 FPS
25 FPS
30 FPS
EFF (IN-LB/IN-LB)
24.
20.
16.
12.
8.
4.
0.
200.
300.
400.
500.
600.
700.
CALCULATED TEMPERATURE (DEG F)

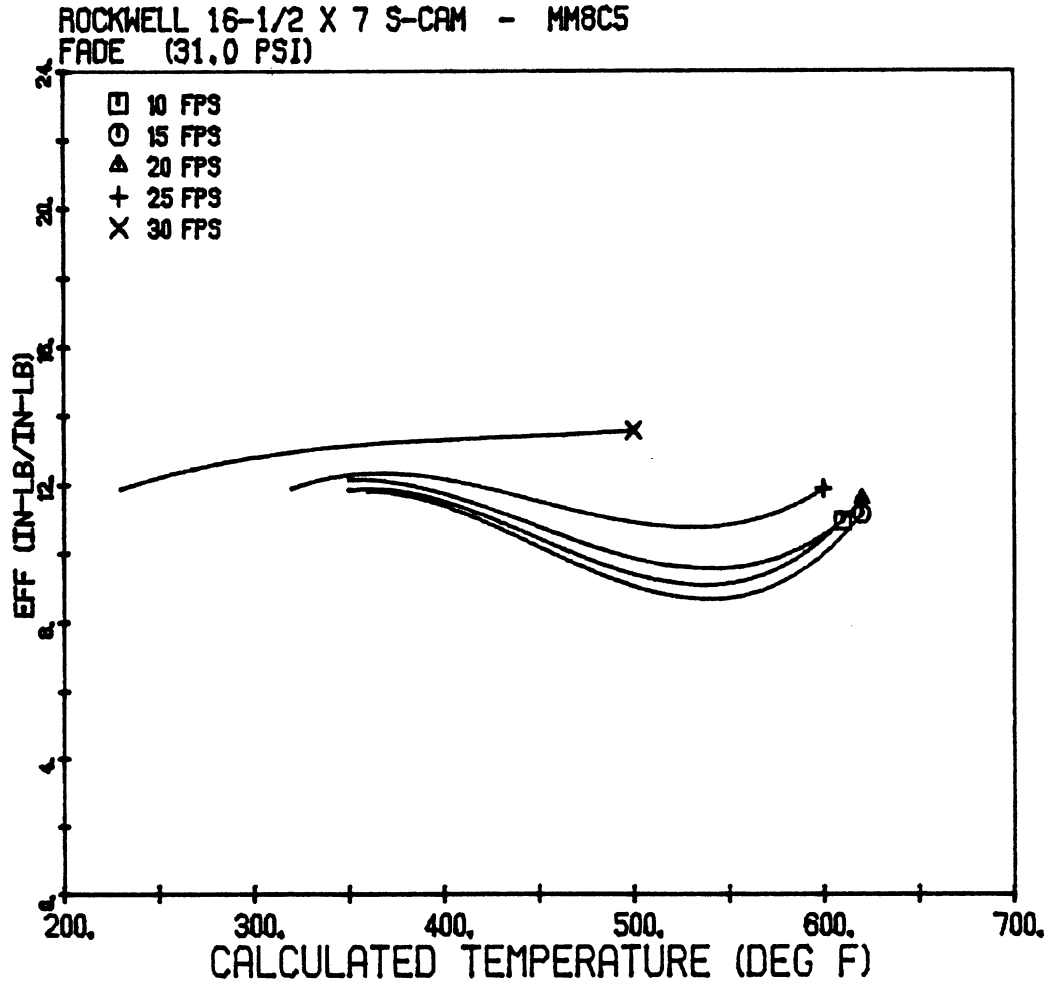
ROCKWELL 16-1/2 X 7 S-CAM - MM8C5
FADE (31.0 PSI)
10 FPS
15 FPS
20 FPS
25 FPS
30 FPS
EFF (IN-LB/IN-LB)
24.
20.
16.
12.
8.
4.
0.
200.
300.
400.
500.
600.
700.
CALCULATED TEMPERATURE (DEG F)

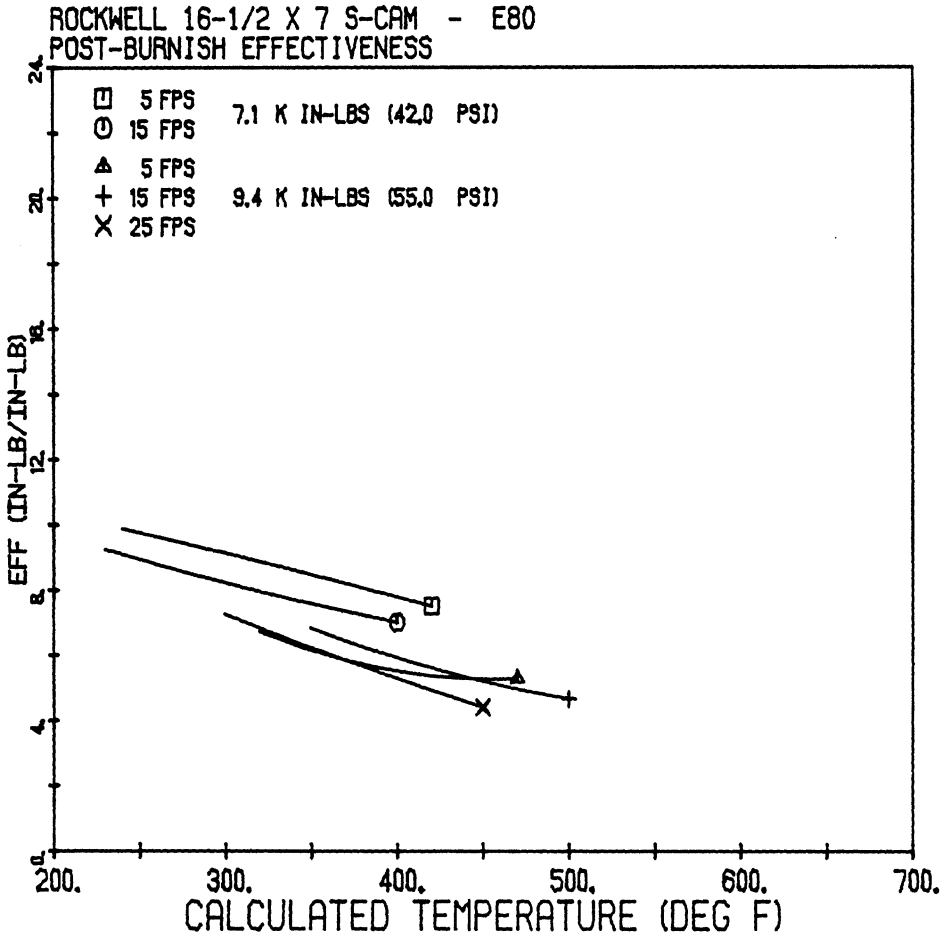
ROCKWELL 16-1/2 X 7 S-CAM - E80
POST-BURNISH EFFECTIVENESS
5 FPS
15 FPS
7.1 K IN-LBS (42.0 PSI)
5 FPS
15 FPS
9.4 K IN-LBS (55.0 PSI)
25 FPS
EFF (IN-LB/IN-LB)
0.
4.
8.
12.
16.
20.
24.
200.
300.
400.
500.
600.
700.
CALCULATED TEMPERATURE (DEG F)

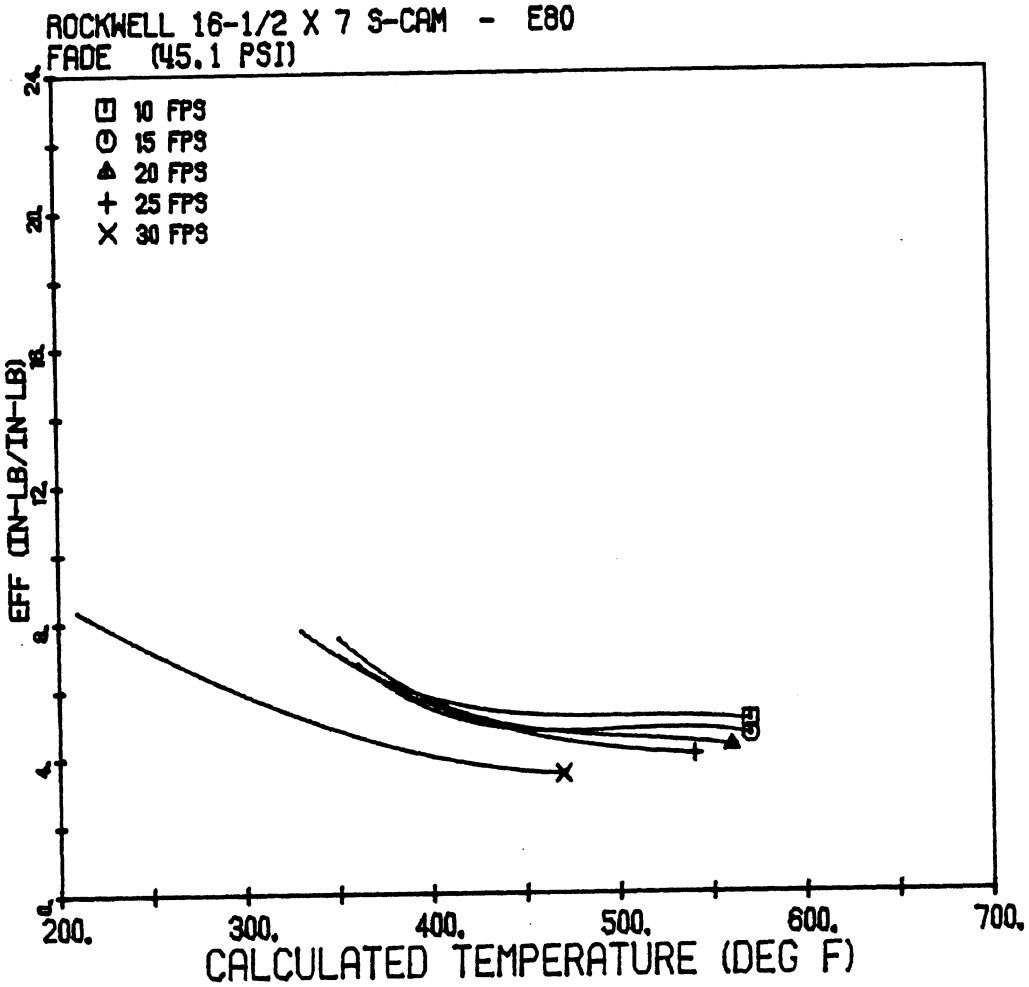
ROCKWELL 16-1/2 X 7 S-CAM - E80
FADE (45.1 PSI)
10 FPS
15 FPS
20 FPS
25 FPS
30 FPS
EFF (IN-LB/IN-LB)
24.
20.
16.
12.
8.
4.
0.
200.
300.
400.
500.
600.
700.
CALCULATED TEMPERATURE (DEG F)

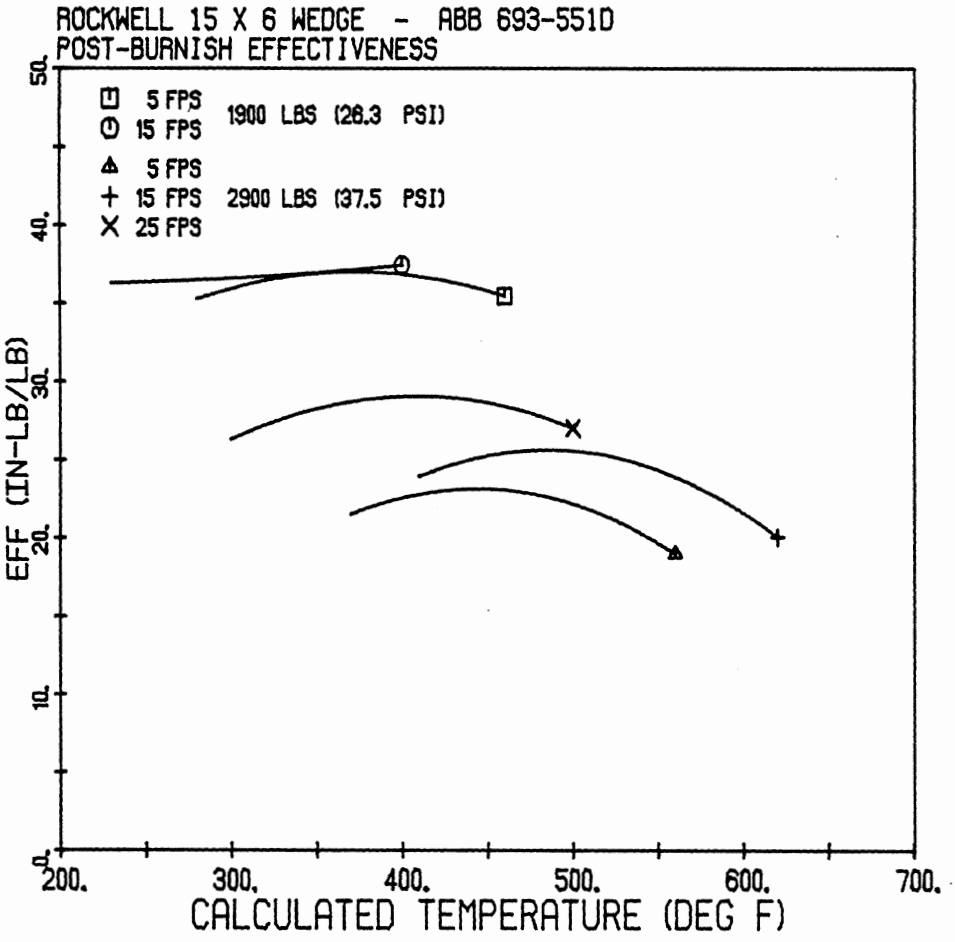
ROCKWELL 15 X 6 WEDGE - ABB 693-551D
POST-BURNISH EFFECTIVENESS
5 FPS
15 FPS
1900 LBS (26.3 PSI)
5 FPS
15 FPS
2900 LBS (37.5 PSI)
25 FPS
EFF (IN-LB/LB)
0.
10.
20.
30.
40.
50.
200.
300.
400.
500.
600.
700.
CALCULATED TEMPERATURE (DEG F)

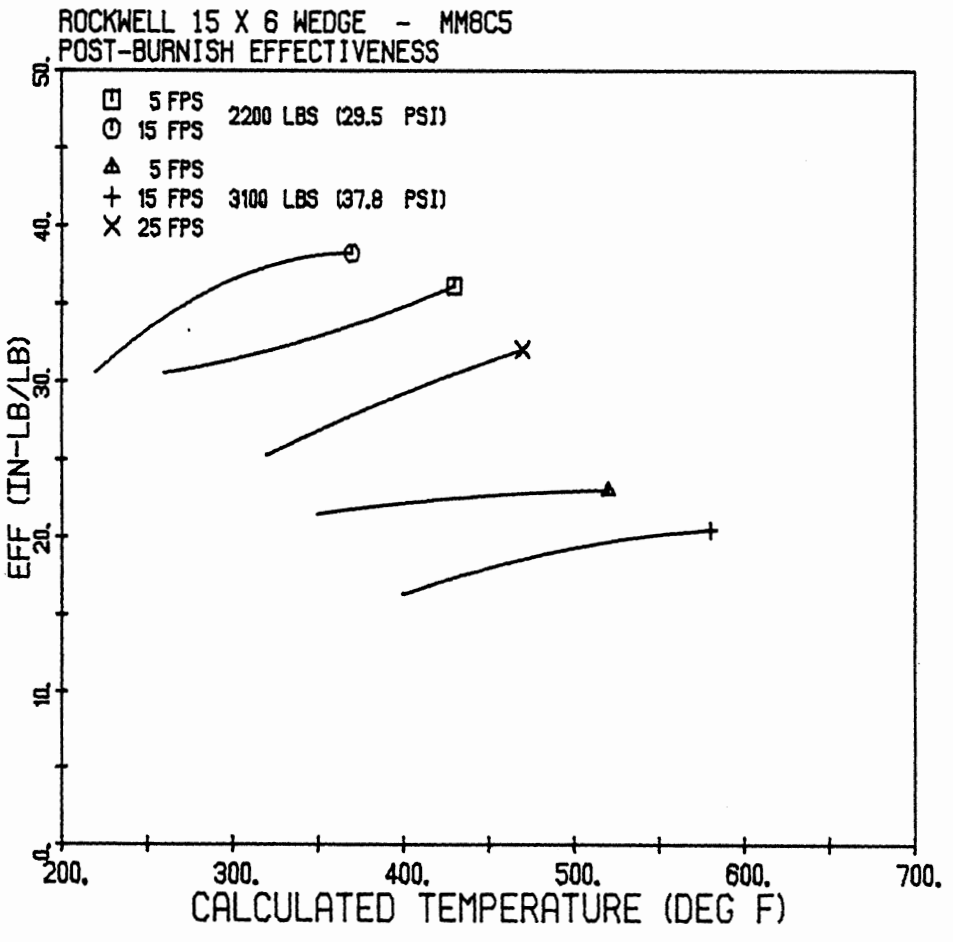
ROCKWELL 15 X 6 WEDGE - MM8C5
POST-BURNISH EFFECTIVENESS
5 FPS
15 FPS
2200 LBS (29.5 PSI)
5 FPS
15 FPS
3100 LBS (37.8 PSI)
25 FPS
EFF (IN-LB/LB)
0.
10.
20.
30.
40.
50.
200.
300.
400.
500.
600.
700.
CALCULATED TEMPERATURE (DEG F)

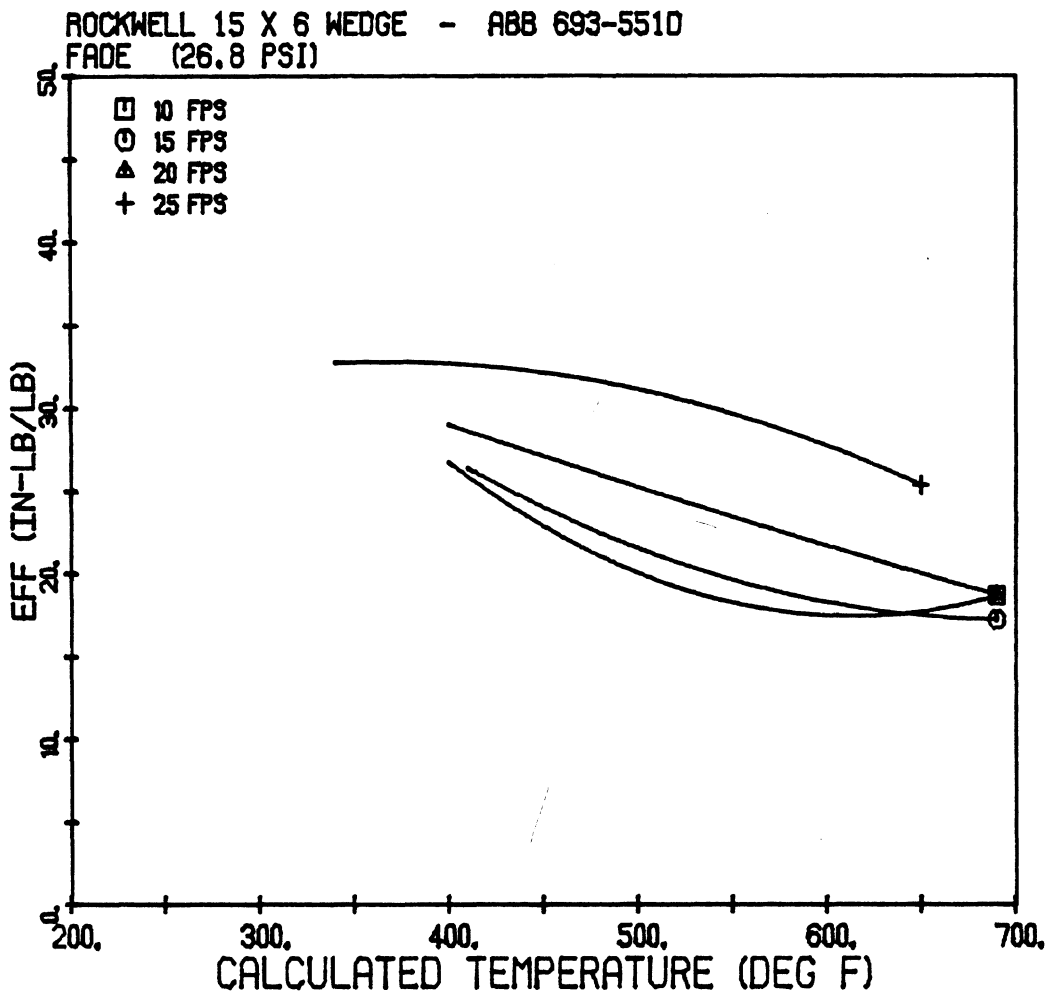
ROCKWELL 15 X 6 WEDGE - ABB 693-5510
FADE (26.8 PSI)
10 FPS
15 FPS
20 FPS
25 FPS
EFF (IN-LB/LB)
0.
10.
20.
30.
40.
50.
200.
300.
400.
500.
600.
700.
CALCULATED TEMPERATURE (DEG F)

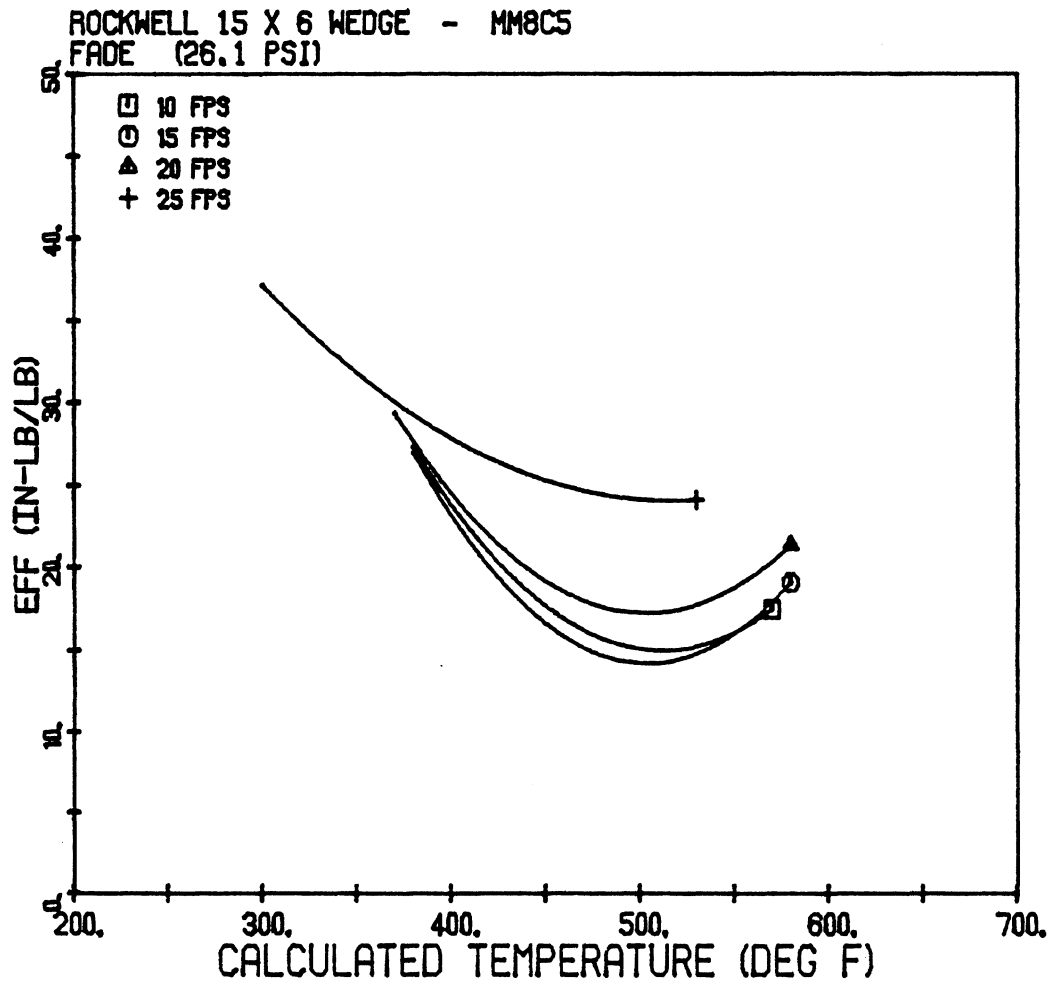
ROCKWELL 15 X 6 WEDGE - MM8C5
FADE (26.1 PSI)
10 FPS
15 FPS
20 FPS
25 FPS
EFF (IN-LB/LB)
0.
10.
20.
30.
40.
50.
200.
300.
400.
500.
600.
700.
CALCULATED TEMPERATURE (DEG F)

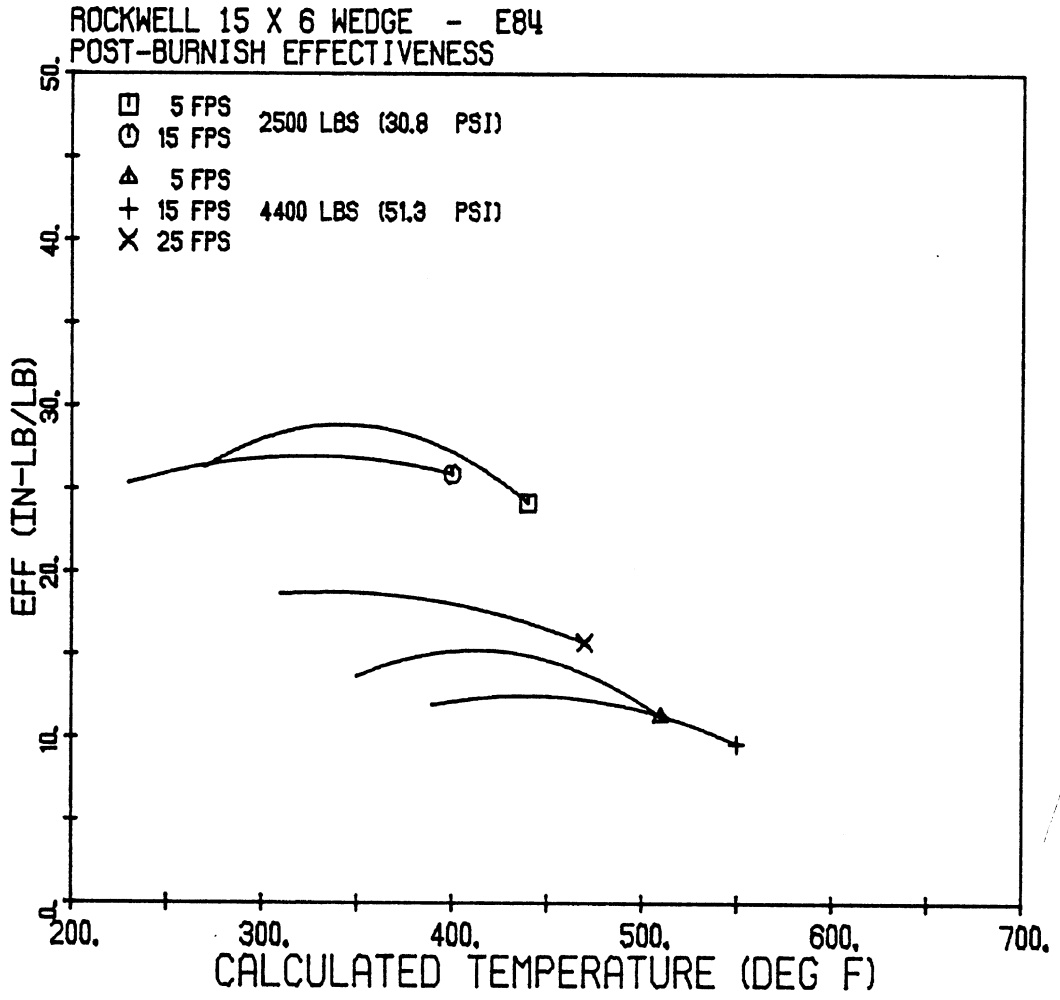
ROCKWELL 15 X 6 WEDGE - E84
POST-BURNISH EFFECTIVENESS
5 FPS
15 FPS
2500 LBS (30.8 PSI)
5 FPS
15 FPS
4400 LBS (51.3 PSI)
25 FPS
EFF (IN-LB/LB)
50.
40.
30.
20.
10.
0.
200.
300.
400.
500.
600.
700.
CALCULATED TEMPERATURE (DEG F)

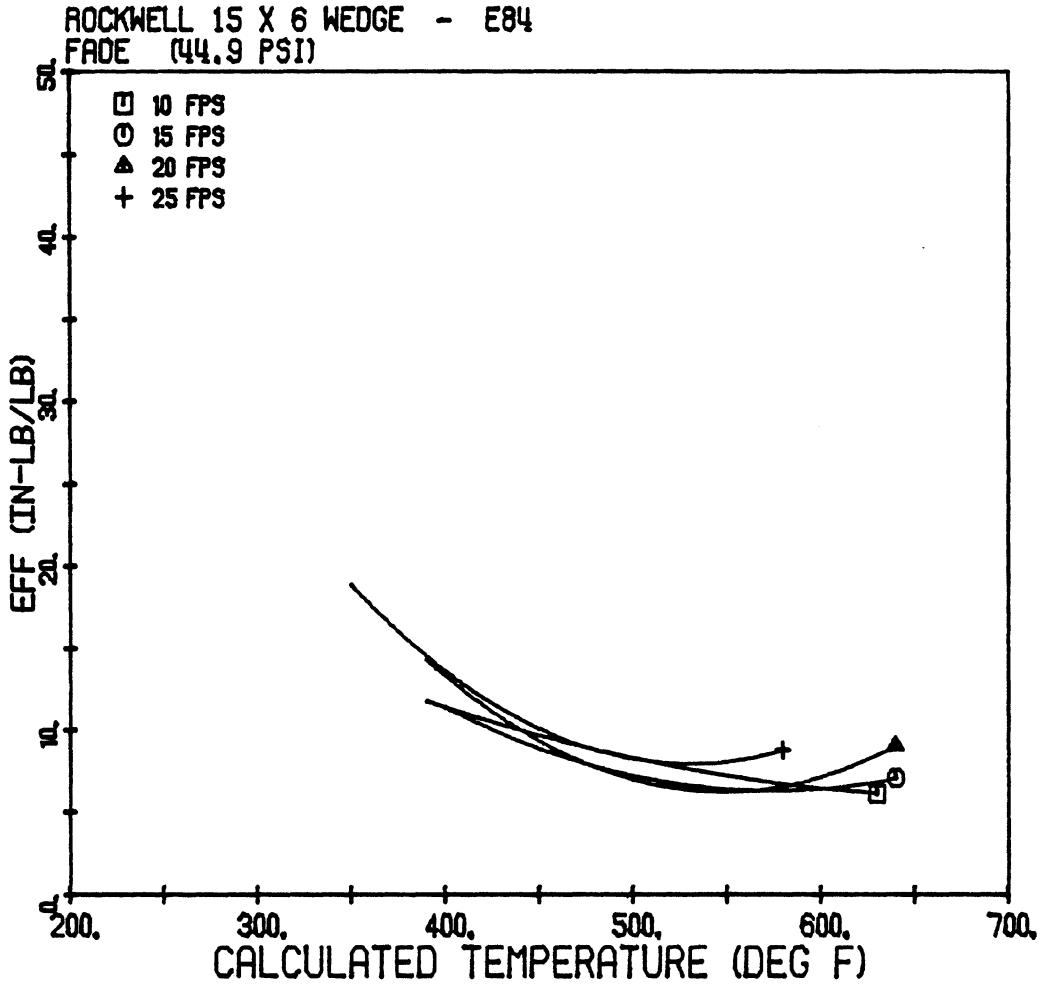
ROCKWELL 15 X 6 WEDGE - E84
FADE (44.9 PSI)
10 FPS
15 FPS
20 FPS
25 FPS
EFF (IN-LB/LB)
50.
40.
30.
20.
10.
0.
200.
300.
400.
500.
600.
700.
CALCULATED TEMPERATURE (DEG F)